Journal of Neurochemistry JNC The Official Journal of the International Society for Neurochemistry

Adult hippocampal neurogenesis and social behavioural deficits in the R451C Neuroligin3 mouse model of autism are reverted by the antidepressant Fluoxetine

Journal:	*Journal of Neurochemistry*
Manuscript ID	JNC-2022-0347.R1
Manuscript Type:	Original Article
Date Submitted by the Author:	n/a
Complete List of Authors:	Gioia, Roberta; University of Rome La Sapienza Seri, Tommaso; University of Rome La Sapienza Diamanti, Tamara; University of Rome La Sapienza Fimmanò, Stefania; University of Rome La Sapienza Vitale, Marina; University of Rome La Sapienza Ahlenius, Henrik; Lund University Hospital Kokaia, Zaal; Lund University Hospital, Stem Cell Center Tirone, F.; Institute of Biochemistry and Cell Biology National Research Council Monterotondo Branch Micheli, Laura; Institute of Biochemistry and Cell Biology National Research Council Monterotondo Branch Biagioni, Stefano; University of Rome La Sapienza, Biologia e Biotecnologie "Charles Darwin" Lupo, Giuseppe; University of Rome La Sapienza Rinaldi, Arianna; University of Rome La Sapienza DE JACO, Antonella; University of Rome La Sapienza, Biology and Biotechnology "C. Darwin" CACCI, Emanuele; University of Rome La Sapienza, Biology and Biotechnology
Keywords:	Adult neural stem cells, Neurogenesis, Post-synaptic proteins, Neurodevelopmental disorders, Sociability
Area/Section:	Brain Development & Cell Differentiation

Title

Adult hippocampal neurogenesis and social behavioural deficits in the R451C Neuroligin3 mouse model of autism are reverted by the antidepressant Fluoxetine

Authors contribution

Gioia R[1], Seri T[1,2], Diamanti T[1] , Fimmanò S[1], Marina Vitale[1], Ahlenius H[3], Kokaia Z[4], Tirone F[5], Micheli L[5], Biagioni S[1], Lupo G[1], Rinaldi A[1,6], De Jaco A[1,6]*, Cacci E[1,6]*

Affiliation

1. Dept of Biology and Biotechnology “Charles Darwin”, Sapienza, University of Rome
2. PhD program in Behavioral Neuroscience, Sapienza University of Rome
3. Lund University, Faculty of Medicine, Department of Clinical Sciences Lund, Neurology, Stem Cells, Aging and Neurodegeneration, Lund, Sweden; Lund Stem Cell Center, Lund, Sweden
4. Lund Stem Cell Center, Department of Clinical Sciences, Lund University Hospital, 22184 Lund, Sweden
5. Institute of Biochemistry and Cell Biology, National Research Council, Rome, Italy
6. Centre for Research in Neurobiology “D. Bovet”, Sapienza University of Rome

*Co-corresponding authors

Cacci Emanuele: emanuele.cacci@uniroma1.it
Antonella De Jaco: antonella.dejaco@uniroma1.it

Abstract

Neuron generation persists throughout life in the hippocampus but is altered in animal models of neurological and neuropsychiatric diseases, suggesting that disease-associated decline in cognitive and emotional hippocampal-dependent behaviours might be functionally linked with dysregulation of post-natal neurogenesis.
Depletion of the adult neural stem/progenitor cell (NSPCs) pool and neurogenic decline have been recently described in mice expressing synaptic susceptibility genes associated with autism spectrum disorder (ASDs).
To gain further insight into mechanisms regulating neurogenesis in mice carrying mutations in synaptic genes related to monogenic ASDs, we used the R451C Neuroligin3 knock-in (Nlgn3 KI) mouse, which is characterized by structural brain abnormalities, deficits in synaptic functions, and reduced sociability.
We show that the number of adult-born neurons, but not the size of the NSPC pool, was reduced in the ventral dentate gyrus in knock-in mice. Notably, this neurogenic decline was rescued by prolonged administration of the antidepressant fluoxetine. Sustained treatment also improved KI mice sociability and increased the number of c-Fos active adult-born neurons, compared with vehicle-injected KI mice.

Our study uncovers neurogenesis-mediated alterations in the brain of R451C KI mouse, showing that the R451C Nlgn3 mutation leads to lasting, albeit pharmacologically reversible, changes in the brain, affecting neuron formation in the adult hippocampus. Our results suggest that fluoxetine can ameliorate social behaviour in KI mice, at least in part, by rescuing adult hippocampal neurogenesis, which may be relevant for the pharmacological treatment of ASDs.

Introduction

In the mammalian brain, type 1 cells (also known as radial glia-like cells) located in the subgranular zone (SGZ) of the dentate gyrus (DG) of the hippocampus produce immature neurons that over the course of several weeks mature and become functionally integrated into the pre-existing hippocampal circuitries (Zhao, Deng, & Gage, 2008); (Kuhn, Toda, & Gage, 2018); (Kempermann et al., 2018); (Jessberger & Gage, 2014).

Adult hippocampal neurogenesis (AHN) is involved in spatial and contextual learning and emotional and social behaviours. For example, genetic ablation of AHN in mice kept under restraint conditions caused increased anxiety and depressive-like behaviour (Snyder, Soumier, Brewer, Pickel, & Cameron, 2011); (Tunc-Ozcan et al., 2019); (Anacker et al., 2018), whereas genetic approaches leading to increased AHN exerted opposite effects (Hill, Sahay, & Hen, 2015). Stimulation of the entorhinal cortex-DG circuitry causes an antidepressant effect in mice that mechanistically relies on AHN (Yun et al., 2018). Moreover, some of the effects of the antidepressant fluoxetine, a selective serotonin reuptake inhibitor, involve AHN modulation and adult-born neuron activation (David et al., 2009); (Santarelli et al., 2003); (Tunc-Ozcan et al., 2019); (Surget et al., 2011). Concerning social behaviour, AHN modulation by genetic or chemogenetic approaches in mice exposed to chronic social defeat stress, produced social behavioural changes (Anacker et al., 2018); (Opendak et al., 2016) .

More recently, AHN defects have gained attention as possible contributors to neurodevelopmental disorders, including ASDs (Bicker, Nardi, Maier, Vasic, & Schmeisser, 2021). ASDs are characterized by impairment in social interaction and communication, cognitive deficits, anxiety, repetitive/stereotypic behaviours, and are often accompanied by seizures and atypical morphological brain structure (Goh & Peterson, 2012); (Postema et al., 2019). The pathogenesis of ASDs involves the occurrence of aberrant neuronal network formation and remodelling during brain development that underlies the early onset of pathological symptoms (Polšek, Jagatic, Cepanec, Hof, & Simić, 2011). The persistence of such alterations in adulthood might also affect neuronal plasticity linked to adult neurogenesis, although this remains to be elucidated.

Consistently, the black and tan brachyury mouse strain (BTBR mice), an animal model of idiopathic autism displaying repetitive behaviour and deficits in social interaction (Ellegood & Crawley, 2015); (Meyza et al., 2013), exhibits a strong reduction in both progenitor proliferation and newly born neurons in the adult hippocampus (Stephenson et al., 2011). Experimental rescue of AHN in BTBR mice was shown to ameliorate mice sociability (Cai et al., 2019). AHN impairment was also observed in two mouse strains carrying mutations in the ASDs-risk genes *Cntnap2* and *Shank3,* encoding for synaptic proteins. Both mouse strains show significant reductions in the number of $GFAP^+$ radial glia-like cells and Dcx^+ immature neurons in the ventral DG (Cope et al., 2016). AHN inhibition in transgenic GFAP–thymidine kinase rats produces behavioural changes in social preference similar to those

observed with the social disruption paradigm (Opendak et al., 2016), suggesting that the decreased sociability observed in Shank3 mutant mice may depend on AHN impairment (Cope et al., 2016).

To assess whether AHN impairment is a hallmark in different ASDs mouse models and to understand how AHN and ASDs affect each other, it is crucial to extend these analyses to additional models.

In this study, we investigated AHN in the R451C Neuroligin 3 knock-in (*Nlgn3* KI) mouse model, reproducing the human mutation found in an ASD-affected Swedish family (Jamain et al., 2003).

Nlgn3 belongs to a family of postsynaptic cell adhesion proteins that binds the presynaptic partner neurexin and are involved in specialization, function, and plasticity of synapses (Südhof, 2008). Nlgn3 is expressed at both the excitatory and inhibitory synapses (Budreck & Scheiffele, 2007), while two other members, Nlgn1 and Nlgn2, are localized predominantly at excitatory and inhibitory synapses, respectively (Chubykin et al., 2007); (Varoqueaux, Jamain, & Brose, 2004). The R451C Nlgn3 KI mice show behavioural alterations related to ASDs. Specifically, these mice display repetitive behaviours and a reduction in the time spent exploring an unfamiliar caged mouse during the three-chamber test, indicating a social interaction deficit (Rothwell et al., 2014); (Etherton et al., 2011).

There is limited evidence of involvement of *Nlgns* involvement in AHN (Schnell, Bensen, Washburn, & Westbrook, 2012); (Schnell, Long, Bensen, Washburn, & Westbrook, 2014); (Krzisch et al., 2017); (Xu et al., 2019) and no data are available in the context of *Nlgn* mutations associated with ASDs.

In this study, we show a reduction of adult-born neurons in the ventral DG of R451C Nlgn3 KI mice in comparison with wild-type (WT) mice. Intriguingly, sustained administration of the antidepressant drug fluoxetine rescued AHN and improved sociability of *Nlgn3* KI mice. These results suggest that AHN impairment contributes, at least partially, to the altered sociability in the R451C Nlgn3 mouse model and point to AHN as a potential target for the pharmacological treatment of ASDs.

Methods and Materials

Experimental Subjects

B6;129-Nlgn3tm1Sud/J knock-in mice (R451C KI) and parental strain (WT) were a kind gift from Dr. Andrea Barberis (Italian Institute of Technology, Genova). All experimental procedures were performed on male littermate mice, obtained from mating either WT or R451C KI male mice with heterozygous females (Nlgn3 is an X-linked gene), which produced 50:50 WT and R451C KI offspring (L Trobiani et al., 2018). Mice were provided with *ad libitum* food and water and kept on at 12 h light/12 h dark cycle at a temperature of 20 ± 1 °C. All analyses were performed on two-month-old (P60) or three months-old mice and were tested between 9.00 a.m. and 16.00 p.m. For genotyping, the R451C mutation was detected by PCR amplification of the genomic DNA, extracted from the mouse tail using primers previously described (Tabuchi et al., 2007). The DNA was used for PCR amplification of the insertion site of the loxP site in the *NLGN3* gene (F 5'-TGTACCAGGAATGGGAAGCAG-3'; R 5'-GGTCAGAGCTGTCATTGTTCAC-3'). Amplified DNA shows a 40bp size shift for the R451C-NLG3 genomic DNA in comparison to WT.

Ethical Approval

Mouse sacrifice was done according to the animal protocol and to the current Italian law (D.lgs. 26/2014). All experimental procedures and protocols were approved by the Ethical Committee for Animal Research of the Italian Ministry of Public Health (Authorization N. 541/2016-PR; 351/2021-PR).

Experimental Design and Procedures

Immunohistochemical and social behavioural analyses after BrdU and Fluoxetine injection

BrdU was used to study cell proliferation and hippocampal neuron formation in 1-month-old mice (P40-P42), according to a previously established protocol (Taupin, 2007).
In order to assess neural stem progenitor cell proliferation, intraperitoneal (i.p.) injections of bromodeoxyuridine (BrdU, 150 mg/Kg i.p. 10 µL/g, Sigma-Aldrich, S.Louis, MO, USA) were given three times daily and mice sacrificed two hours after the last injection.
In order to quantify adult-born neuron formation, mice received a single daily i.p. BrdU injection for five days and then were sacrificed two or eight weeks after the last administration (see experimental timeline, Figure 1A).
In order to assess the effect of the antidepressant fluoxetine on both AHN and mice behaviour, animals were administered with BrdU during the first five days in combination with fluoxetine or vehicle; Fluoxetine hydrochloride (10 mg/Kg, 10 µL/g in 0.9% NaCl; Alfa Aesar) or vehicle (0.9% NaCl) were administered daily by i.p. injections along 20 consecutive days as shown in the scheme (Figure 3). Animals were then either directly sacrificed for AHN immunohistochemical quantification or analysed 24 hrs after the last fluoxetine injection for social behaviour, and then sacrificed to assess adult-born neuron activation.

For immunohistochemical analyses, mice were deeply anesthetized by i.p. injection of Zoletil (Tiletamine-Zolazepam 1:1 100 mg/Kg) and Rompun (Xilazine 20 mg/Kg), brains were collected after trans-cardiac perfusion with PBS followed by 4% paraformaldehyde (PFA Sigma-Aldrich) in PBS (pH 7,5; 137 mM NaCl, 2.7 mM KCl, 1.4 mM KH_2PO_4, 6.45 mM Na_2HPO_4), and kept overnight in PFA 4%, equilibrated in sucrose/saline 30% for 2 days at 4 °C and then cryopreserved at -80°C until the use.

Immunohistochemistry and cell quantification on hippocampal sections

Immunohistochemistry was performed on serial free-floating coronal sections cut at 30 µm thickness in a freezing microtome (Leica) from brains cryopreserved at -80°C. Free-floating sections were immunolabeled for single or multiple markers using fluorescent methods.

Quiescent and activated NSCs, progenitor cells, newly-formed neurons and activated neurons were identified using specific combinations of the following primary antibodies: rabbit polyclonal anti Ki67 antibody (catalog number ab15580; Abcam; 1:200 dilution), mouse monoclonal anti GFAP antibody (catalog number G6171; Sigma; 1:500 dilution), goat polyclonal antibody against Sox2 (catalog number 239218; Abcam; 1:300 dilution); goat polyclonal anti DCX antibody (catalog number SC-8066; Santa Cruz; 1:300 dilution); mature

differentiated neurons were identified using mouse monoclonal anti NeuN antibody (catalog number MAB377; Millipore; 1:200 dilution); rabbit polyclonal anti c-Fos antibody (catalog number D82C12; Cell Signalling Technology; 1:1000 dilution); rat primary monoclonal anti BrdU antibody (catalog number MCA2060T; Serotech; 1:400 dilution)

Free-floating sections were pre-treated with 0,1 M glycine (Sigma-Aldrich) in PBS for 10 minutes, and with Citrate Buffer 10 mM pH 6 for 15 minutes at 50 °C. In order to reduce the background DCX staining was performed after a pre-treatment with NaBH4 0,5% in H_2O for 10 min depending on the antibody used. For BrdU detection, a DNA denaturing step with 2N HCl 40 min at room temperature, followed by 0.1 M sodium borate buffer pH8.5 for 10 min was performed before the next step.

Tissue sections were blocked with a buffer solution (Tris-buffered saline) containing 5% donkey normal serum and 0,1 % Triton X-100, for not less than 1 hour and then incubated overnight at 4°C with the specific primary antibodies diluted in the appropriate blocking solutions.

For BrdU staining, the rat primary monoclonal anti BrdU antibody (MCA2060T, Serotech, 1:400) was diluted in a solution containing 5% normal donkey serum, 0,1% Triton X-100, and 0,03% Tween20.

Secondary antibodies were all from Jackson ImmunoResearch (used 1:200) as follows: a donkey anti-rat antiserum Cy3-conjugated (BrdU labelling); a donkey anti-goat antiserum cy3-conjugated (DCX labelling) and Alexa-647 (Sox2 labelling); a donkey anti-rabbit antiserum conjugated to Alexa-488 (Ki67 labelling) and cy3-conjugated (c-Fos labelling). Nuclei were counterstained by Hoechst 33342 (Sigma-Aldrich; 1 µg/ml in PBS).

Confocal single plane images and Z-stacks with orthogonal projections of the immunostained sections were obtained using a TCS SP5 confocal laser scanning microscope (Leica Microsystems).

The quantification analysis was performed considering that adult-born DG granule cells (GCs) regulate emotional and social behaviour or contextual and spatial learning depending on their position along the longitudinal axis, described as dorsoventral in rodents (Kheirbek et al., 2013); (Strange, Witter, Lein, & Moser, 2014); (Fanselow & Dong, 2010). We quantified separately adult-born neurons into dorsal and ventral segments along the longitudinal axis of the DG of R451C Nlgn3KI and WT mice. We defined 8 continuous 30-µm-thick coronal sections as a block of 240 µm-length and divided the whole DG (longitudinal length of 2,88 mm) into 12 blocks, six blocks (from 1 to 6) categorized as the dorsal DG and six blocks (from 7 to 12) categorized like the ventral DG as shown Supplementary figure 1. For quantification analysis, we examined one-in-eight series of 30µm free-floating coronal sections that are representative of each block. To obtain the total estimated number of cells the average number of 12 sections was multiplied by the total number of sections (≅96 for the whole DG, ≅48 for ventral and dorsal DG) comprising the entire dentate gyrus (2.88 mm 240µm apart) as previously described (Gould, Beylin, Tanapat, Reeves, & Shors, 1999); (Jessberger, Römer, Babu, & Kempermann, 2005) .

Three-chamber Test and adult-born neuron activation assessment

The three-chamber test was performed in a rectangular Plexiglas arena (70x20x20 cm) divided into three chambers (each 23x20x20 cm) that communicate by removable doors

situated on the walls of the center chamber. Two Plexiglas perforated cylinder containers (with 8 cm diameter) are placed in the middle of each side chamber to contain the unfamiliar mouse. Mice were subjected to the three-chamber test 24 hrs after the last fluoxetine (or vehicle) administration (see method details-fluoxetine administration). The subject mouse (8-12 weeks old) was placed in the empty arena for the habituation phase, which consisted of 10 min of free exploration. Subsequently, the mouse was kept in the center chamber by closing the removable doors and the two cylinders were placed in the side chambers, one was left empty and the other one contained a non-familiar social stimulus (novel WT male mice, 6-8 weeks-old). The doors were removed, and the subject mouse freely explored the arena for 10 min (sociability session). The stimuli mice were habituated to the Plexiglas cylinders during three sessions of 10 min on three non-consecutive days before the experiment. The position of the social stimulus was randomly assigned and counterbalanced. Before the social novelty preference session, the subject mouse was kept a second time in the center chamber to allow the position of a new non-familiar conspecific in the previously empty cylinder. The doors were opened for the second time and the subject mouse explored the arena for 10 min (social novelty preference). After each session all chambers were cleaned with 70% ethanol and dried to prevent olfactory cue bias. The sessions were video-tracked and recorded using Anymaze (Stoelting) and an experimenter blind to the treatment and genotype of the subjects manually scored behaviour by measuring the following parameters: time spent sniffing, time spent in each of the three chambers, latency to the first entry and distance travelled. We analysed each 10 minutes session by dividing it into two 5 minutes parts; in the results, we present only data from the first 5 minutes of each session, in which main differences emerged, as previously shown (Bariselli et al., 2018) .

Animals were sacrificed 1-hour after the end of the task and immunostained for c-Fos (a proxy marker of neuronal activity) and BrdU, as described above. The time point chosen corresponds to the peak of *c-Fos* expression after neuron activation (Kovács, 1998).

Materials

REAGENT or RESOURCE	**SOURCE**	**IDENTIFIER**
ANTIBODIES		
Rabbit anti-Ki67	Abcam	Cat#ab15580; RRID:AB_443209
Rat anti-BrdU	Bio-Rad / Serotec	Cat#MCA2060T,RRID:AB_10015293
Mouse anti-NeuN	Millipore	Cat# MAB377, RRID:AB_2298772
Goat anti-DCX	Santa Cruz Biotecnology	Cat#SC-8066; RRID:AB_2088494

Goat anti-Sox2	Abcam	Cat#239218; RRID: AB_2814791
Mouse anti-GFAP	Sigma	Cat#G6171;RRID: AB_1840893
Rabbit anti-c-Fos	Cell Signalling Technology	Cat#D82C12;RRID: AB_10557109
Donkey anti-rat,Cy3-conjugated	Jackson ImmunoResearch	Cat#712-165-150, RID:AB_2340666
Donkey anti-goat,Cy3-conjugated	Jackson ImmunoResearch	Cat#705-165-003, RID:AB_2340411
Donkey anti-goat,Alexa-647	Jackson ImmunoResearch	Cat#705-605-147;RRID: AB_2340437
Donkey anti-rabbit,Alexa-488	Jackson ImmunoResearch	Cat#711-545-152, RID:AB_2313584
Donkey anti-rabbit, Cy3-conjugated	Jackson ImmunoResearch	Cat#711-167-003, RID:AB_2340606
Donkey anti-mouse,Alexa-488	Jackson ImmunoResearch	Cat#715-545-151, RID:AB_2341099
CHEMICALS, PEPTIDES		
Hoechst 33342	ThermoFisher	Cat#H3570
Bromodeoxyuridine	Sigma-Aldrich	Cat#B9285
Fluoxetine hydrochloride	Alfa Aesar	Cat#J61197
Dako mounting medium	Dako	Cat# S3023
SOFTWARE & OTHER SOURCES		
Prism	GraphPad software	N/A
Nikon Eclipse TE300	Nikon	N/A
TCS SP5 confocal laser scanning microscope	Leica Microsystems	N/A

Statistical analysis

All the experiments were performed at least three times on independent biological samples, as indicated in the figure legends. WT and KI mice were analyzed in equal numbers and were randomly assigned to the experiments, no data or outliers were removed for the statistical analysis. The Student's t-test was used to compare data with normal distribution. The two-way ANOVA was used to estimate the total cell number mean of specific cell subpopulations (determined by immunohistochemistry). The sample size for the behavioural experiment was determined *a priori* based on preliminary results using the software G*Power (effect size=1.8; =0.5, power=0.9)

Time spent sniffing and latency to first entry in the three-chambers test were analyzed by three-way repeated-measures ANOVA with the factors chamber (repeated measure, two levels: stranger1-object or stranger1-stranger2, for sociability and social novelty preference session respectively), genotype (two levels: WT and KI), and treatment (two levels: fluoxetine and vehicle). Time spent in the chamber was analyzed by three-way repeated-measures ANOVA with the factors chamber (repeated measure, three levels: stranger1-center-object or stranger1-center-stranger2 respectively for sociability or social novelty preference session), genotype (two levels: WT and KI), and treatment (two levels: fluoxetine and vehicle). When appropriate, further comparisons were carried out by Fisher's PLSD post-hoc test.

When data were expressed as percentage ratio, the Kruskal-Wallis test, which accounts for the assumption of non-normal distribution, was used to compare the effects of fluoxetine on genotypes, followed by Dunn's post-hoc test for further comparisons. All analyses were performed using Prism8 (Graph-Pad 8 Software Inc.). Data were expressed as mean values ± SEM. Differences were considered statistically significant at $*p \leq 0.05$, and $**p \leq 0.01$, $***p \leq 0.001$.

Results

Decreased number of adult-born neurons in the DG of R451C *Neuroligin3* KI mice

In order to quantify AHN, adult R451C Nlgn3 KI and WT mice (P42) were injected daily with BrdU for five days (150 mg/kg i.p.) and then sacrificed two weeks after the last injection (P60) (Figure 1A). Fixed hippocampal coronal sections were stained for BrdU and either the neuroblast marker DCX (Figure 1B,C) or the post-mitotic neuronal marker NeuN (Figure 1D,E). The number of newly-formed neurons was analyzed in the dorsal and ventral DG, involved in regulation of learning and spatial memory, and in anxiety-like and emotional behavior, respectively (Cameron & Glover, 2015); (Anacker & Hen, 2017). We observed reduced numbers of both BrdU/DCX (Figure 1C) and BrdU/NeuN double-positive cells (Figure 1E) in the ventral DG of KI mice, relative to WT, while no differences were observed in the dorsal DG.

Adult-born neurons were additionally counted eight weeks after the last BrdU injection. Also at this time point, a significant reduction in the number of BrdU/NeuN double-positive cells was observed in the ventral but not in the dorsal DG of KI mice in comparison with WT mice (Figure 1F). These data demonstrate that the R451C Nlgn3 mutation causes a consistent and lasting decrease in the number of newborn neurons, indicating that AHN is reduced in KI mice and that this decrease is unlikely to be explained by a delay in neuronal differentiation/maturation.

Progenitor subpopulation type2b/type3 was reduced in the DG of R451C *Neuroligin3* KI mice

To dissect the potential mechanisms underpinning the reduction in neurogenesis observed in R451C Nlgn3 mice, we looked first at overall DG proliferation. Two-month-old mice received three injections of BrdU at two hours intervals and were sacrificed two hours after the last injection (see scheme Supplementary Figure 2A). DG proliferation was studied by quantifying the number of cells positive for either BrdU or Ki67 (a marker of cells engaged in cell cycle progression) in the ventral and in the dorsal DG subregions. No difference between the two genotypes was observed (Supplementary Figure 2B,C).
As BrdU or Ki67 staining does not allow to unequivocally distinguish the identity of proliferating cells, the differential expression of key markers was used to identify different stem cell and progenitor subpopulations. According to previously established methods (Kempermann, Jessberger, Steiner, & Kronenberg, 2004), hippocampal sections were stained by combining antibodies against specific markers of the following cell types: quiescent type 1 cells ($Sox2^+/GFAP^+/ Ki67^-$), activated type 1 cells ($Sox2^+/GFAP^+/ Ki67^+$), type 2a cells ($Sox2^+/GFAP^-/Ki67^+$) and type 2b-Type3 cells ($Ki67^+/DCX^+$). The number of type 1 quiescent, type1 activated and type 2a subpopulations did not differ between R451C Nlgn3KI and WT mice, neither in the ventral nor in the dorsal DG (Figure 2A,B,C,D). In contrast we observed a significant reduction of Type 2b-Type3 cells ($Ki67^+/DCX^+$) in the DG of R451C Nlgn3 KI as compared to WT (Figure 2 E,F). These data suggest that, mechanistically, a reduction of the neuroblast proliferation may be responsible for the decreased AHN of KI animals.

Fluoxetine rescues neurogenesis in the hippocampus of R451C *Neuroligin3* KI mice

In order to evaluate whether the impaired neurogenesis in Nlgn3 KI mice could be rescued, we injected mice with fluoxetine (FLX), a serotonin-reuptake inhibitor, which is known to promote hippocampal neurogenesis (Zhou, Lee, Ro, & Suh, 2016); (David et al., 2009); (Santarelli et al., 2003). Two-month-old mice were treated daily with FLX (10mg/kg i.p. 10 µl/g) or vehicle (VEH) over 20 consecutive days. During the first five days of FLX treatment, mice also received one BrdU injection per day (150 mg/kg i.p. 10 µl/g) (see timeline, Figure 3A). This protocol enables the detection of 15-to 20-days-old newly formed neurons.
We found that the number of $BrdU^+/NeuN^+$ adult-born neurons in the ventral DG of FLX-treated KI mice reached levels comparable to those observed in WT mice, injected either with VEH or FLX (Figure 3 C), indicating that the treatment with FLX rescues ventral hippocampal neurogenesis in R451C Nlgn3 mice. Notably, FLX did not affect neurogenesis in WT animals using the same experimental conditions (Figure 3 B).

Fluoxetine rescues the social interaction deficits in R451C *Neuroligin3* KI mice

Several studies have described social interaction deficits in R451C Nlgn3 KI mice that are related to the autistic phenotype (Tabuchi et al., 2007); (Etherton et al., 2011); (Jaramillo, Liu, Pettersen, Birnbaum, & Powell, 2014). Since FLX has been shown to ameliorate sociability in other mouse models of ASDs (Chadman, 2011); (Uutela et al., 2014); (Payet et al., 2018), we tested whether the social deficits caused by the R451C mutation could be

ameliorated by treatment of KI mice with FLX (see scheme in Figure 3A). Social behaviour was studied by the three-chamber test one day after the end of the treatment.

Sociability and social novelty preference were assessed by measuring the time spent sniffing either the object or the stranger and either the familiar stranger or the novel stranger (Figure 4 A,D); the time spent in the three chambers (Figure 4 B,E); and the latency to the first entry in the side chambers (Figure 5 C,F).

During the sociability session, VEH-treated WT mice spent more time sniffing the stranger than the object, while VEH-treated KI mice did not show any difference between time spent sniffing the object or the stranger, indicating a sociability impairment (Figure 4 A). R451C KI mice spend less time interacting with a novel caged adult, while they did not change the time of interaction with a novel inanimate object, in agreement with previous results (Tabuchi et al., 2007); (Jaramillo et al., 2014); but see also (Chadman et al., 2008); (Etherton et al., 2011). The treatment of KI mice with FLX increased the time spent sniffing the stranger mouse in comparison to VEH-injected mice, indicating a preference for the stranger. No differences were observed between WT VEH and WT FLX groups. These results indicate an increased social behaviour in response to FLX, which is specifically restricted to the KI genotype (Figure 4 A). The time spent in the three chambers during the sociability session showed that KI VEH mice spent more time in the object chamber than in the stranger chamber, and they spent less time in the stranger chamber with respect to WT VEH mice confirming a sociability impairment. FLX significantly increased the time that the KI mice spent in the stranger chamber and reduced the time that they spent in the center chamber with respect to the vehicle group (Figure 4 B). Interestingly, besides spending more time in the center chamber, KI VEH mice also showed increased latency to the first entry in the stranger chamber compared to WT VEH mice, which was significantly decreased by FLX treatment (Figure 4 C).

During the three-chamber test locomotor activity was also measured in KI and WT mice, expressed as the distance travelled in the different chambers. In the sociability session the total distance travelled increased both in treated and untreated KI mice with respect to the WT (total distance: WT VEH=24.3±1.5 m, WT FLX= 23±1.2 m, KI VEH= 29.3±3.7 m, KI FLX= 32.9±2 m; effect of genotype: $F(1,32)=9.75$, $p\leq0.01$). However, while both KI VEH and KI FLX mice showed increased locomotor activity in the object chamber compared to WT, fluoxetine-treated KI mice also showed increased locomotor activity in the stranger chamber compared to vehicle-treated mice (Supplementary Figure 3A).

During the subsequent social novelty preference session, both WT and KI mice spent more time in the stranger 2 chamber and sniffing the stranger 2 (Figure 4 D,E). The latency to the first entry was similar between the two chambers with either stranger 1 or stranger 2 (Figure 4F). Furthermore, no difference was observed in distance travelled between the genotypes either in presence or in the absence of fluoxetine (Supplementary Figure 3B). Thus, these results do not show differences in the social novelty preference between genotypes and treatments, in accordance with published data (Etherton et al., 2011). Overall, these data indicate that KI mice showed behavioural alterations in sociability
when compared with WT animals, which could be rescued by the treatment with
FLX.

The number of activated adult-born neurons increases in R451C *Neuroligin3* KI mice treated with fluoxetine

To assess whether adult-born neurons get activated we used c-Fos immunohistochemistry to map neuronal activity (Guzowski et al., 2005); (Bernstein, Lu, Botterill, & Scharfman, 2019); (Anacker et al., 2018) in a subset of animals sacrificed one hour after the three-chamber test. c-Fos was detected in neurons identified by the expression of the mature neuronal marker NeuN (Supplementary Figure 4A). Furthermore, double staining for c-Fos and BrdU demonstrated that adult-born neurons were functionally active (Figure 5A)
Confirming our results of increased adult-born neurons (Figure 3), we found that number of $BrdU^+$/$c\text{-}Fos^+$cells was significantly higher in ventral DG of the FLX-treated KI mice than in VEH-injected KI mice, while FLX did not affect the number of $BrdU^+$/$c\text{-}Fos^+$ in the ventral DG of WT animals (Figure 5B). We also found an increased number of $BrdU^+$/$c\text{-}Fos^+$ cells in the dorsal DG of FLX-treated KI animals (Figure 5C), albeit the magnitude was lower compared to the ventral DG. Unexpectedly, fluoxetine reduced the number of $BrdU^+$/$c\text{-}Fos^+$ cells in the dorsal DG of WT animals (Figure 5C).
Overall, these data demonstrate that FLX treatment augmented both the absolute number and the number of activated adult-born neurons in KI animals. The finding that adult-born neurons expressed a marker of neuronal activity upon the three-chamber suggests their potential contribution to animal behaviour.

Discussion

AHN impairment has been observed in animal models of neurological and neuropsychiatric diseases (Sacco, Cacci, & Novarino, 2018); (Toda, Parylak, Linker, & Gage, 2019); (Kang, Wen, Song, Christian, & Ming, 2016), as well as during physiological aging (Lupo, Gioia, Nisi, Biagioni, & Cacci, 2019); (Micheli et al., 2021).
More recently, AHN defects have been studied in animal models of neurodevelopmental disorders, including ASDs (Opendak et al., 2016); (Cai et al., 2019); (Stephenson et al., 2011); (Amiri et al., 2012); (Luo et al., 2010); (Lazarov et al., 2012); (Cope et al., 2016). These studies have highlighted the correlation between adult neurogenesis dysregulation and behavioural deficits associated with ASDs, albeit the causative link remains to be determined. In light of this, a deeper understanding of how ASDs and AHN reciprocally affect each other is needed (Bicker et al., 2021).
We studied regulation of AHN in the R451C Nlgn3 KI mouse model, expressing a previously identified human Nlgn3 mutation associated with a monogenic form of ASD (Jamain et al., 2003); (Tabuchi et al., 2007); (L Trobiani et al., 2018); (Laura Trobiani et al., 2020).
We found that the number of newly generated neurons is reduced in the ventral DG of the KI in comparison to WT mice and that this neurogenic deficit was rescued by sustained pharmacological treatment with the antidepressant FLX. Furthermore, by using c-Fos expression as a proxy of neuronal activity, we also demonstrate that adult-born neurons generated in the ventral DG of FLX-treated KI animals are functionally active during a hippocampal-dependent behavioural task (three chambers test). Notably, FLX treatment not only increased neurogenesis and the number of activated newborn neurons in mice but also improved social behaviour in R451C Nlgn3 KI mice. This suggests a potential neurogenesis-mediated effect of FLX on the behaviour of these mice.

A decrease in the number of immature neurons and progenitor cells with radial glia morphology has been reported in the ventral SGZ of transgenic mice mutated in ASD-associated post-synaptic proteins Cntnap2 and Shank (Cope et al., 2016). Our data show decreased adult-born neuron generation in R451C Nlgn3 KI mice but, at variance with Cntnap2 and Shank3 mouse models, we did not find any difference in the size of the NSC pool (quiescent or activated) or of the Type 2a progenitor subpopulation (Sox2/Ki67-positive). Instead, we report a reduction in the proliferating, neuronal committed, type 2b-type3 neuroblasts subpopulation. The type 2b-type3 pool impairment might be responsible for the decline of newly formed neurons in R451C Nlgn3 KI mice.

Interestingly, the neurogenic decline in the ventral DG of KI mice could be pharmacologically reverted by FLX treatment. The effectiveness of FLX in restoring neurogenesis was previously demonstrated in animals living in a stressful environment or subjected to long-lasting treatments with corticosterone (David et al., 2009; Murray, Smith, & Hutson, 2008; Perera et al., 2011). Serotoninergic receptors have been found widely expressed within the hippocampus, including hilar interneurons, type 2a and type 2b progenitors, immature, and mature neurons (Alenina & Klempin, 2015)), indicating that serotonin-dependent neurogenesis could occur through an indirect mechanism or directly on progenitors. Interestingly, 5HT1A receptor blockage reduced the proliferation of NSPCs in vitro, and selective antagonists of 5-HT1A postsynaptic receptors reduced the number of newly formed cells in the DG (Radley & Jacobs, 2002). As fluoxetine targets the serotonin system by inhibiting serotonin re-uptake, and serotonergic projections are dense in the ventral but not in the dorsal hippocampus (Gage & Thompson, 1980); (Sahay & Hen, 2007), this could explain our results on the major effect of FLX on AHN in the ventral DG.

The different responsiveness to fluoxetine treatment has also been reported to rely on the mouse strain and genetic background (Navailles, Hof, & Schmauss, 2008); (David et al., 2009). Noteworthy, FLX treatment did not exert any effect in WT mice, indicating an increased sensitivity to the drug in KI mice when compared with WT animals. The regional-specific effect of the *Nlgn3* mutation in the excitatory/inhibitory balance and hippocampal circuit reorganization (Etherton et al., 2011); (Tabuchi et al., 2007) might explain the differences between the WT and KI genotypes in terms of FLX-dependent neurogenesis modulation.

The hippocampus is functionally heterogeneous along the dorsoventral axis (Strange et al., 2014), with cognitive and mood/emotional/social behaviour regulation mainly depending on the dorsal and ventral hippocampus respectively. Thus, it is noteworthy that the neurogenesis impairment and FLX pro-neurogenic effects were essentially restricted to the ventral DG of R451C Nlgn3 KI mice. This prompted us to study the FLX effect on the social behaviour of R451C Nlgn3 mice. FLX has been shown to ameliorate behavioural alterations in several mouse models (Chadman, 2011); (Uutela et al., 2014); (Payet et al., 2018) and is used in ASD patients (Aman, Lam, & Van Bourgondien, 2005); (Oswald & Sonenklar, 2007). However, our study is the first to assess FLX effects on the social behaviour of R451C Nlgn3 KI mice

In the absence of FLX, we confirmed sociability impairment in KI mice with respect to the WT, as previously described by Powell and colleagues, reporting no preference for the social target during the three-chamber test (Jaramillo et al., 2014). The Südhof group also reported sociability impairment in the novel home cage activity test, and during the three-chamber test in R451C Nlgn3 KI (Tabuchi et al., 2007); (Etherton et al., 2011). In contrast, other groups did not report any alteration in the sociability of KI mice on hybrid or C57BL6 background; (Chadman et al., 2008); (Etherton et al., 2011). As the genetic background plays an

important role in modifying the penetrance of a particular autism-associated mutation, such difference among studies might reflect differences in the genetic background of KI strains (Jaramillo *et al.,* 2018; Moy *et al.,* 2004). We also reported that the locomotor activity in R451C Nlgn3 KI animals was increased in comparison with WT mice (Burrows et al., 2015). Following FLX treatment R451C Nlgn3 KI, but not WT mice, showed a significant increase in the time sniffing the stranger, and in the time spent in the stranger chamber, as well as a decrease in the latency to the first entry in the stranger chamber.

FLX-mediated social improvement in KI mice was accompanied by an increased number of activated ventral DG adult-born neurons, suggesting that adult-born neurons functionally contributed to R451C Nlgn3 social behaviour. However, both WT and KI mice showed a complex pattern of adult-born neuron activation in the different DG subregions of mice after testing in the three-chamber, possibly mirroring the heterogeneity of the neural inputs to the DG (Catavero, Bao, & Song, 2018).

Based on recent experimental evidence, the idea of a direct relationship between sociability and AHN has been gaining support. For example, it has been reported that AHN ablation produces social preference behavioural changes (Opendak et al., 2016) and chemogenetic inhibition of ventral DG adult-born neuron activity in mice subjected to a chronic defeat social stress produced strong avoidance of a novel mouse in a social interaction test (Anacker et al., 2018). In contrast, mice subjected to a chronic defeat paradigm and conditionally depleted for the pro-apoptotic gene Bax showed increased neurogenesis and increased social interaction time. This study pinpoints that ventral adult-born neurons confer resilience against stress-related abnormal behaviour, including sociability deficits (Anacker et al., 2018). Clearly, our data do not directly demonstrate causality between the fluoxetine-mediated rescue of sociability and neurogenesis in KI mice. For example, fluoxetine antidepressant-like activity has been reported to be mediated either through neurogenesis-dependent or neurogenesis-independent mechanisms, involving the hippocampus and other brain regions (e.g. amygdala, nucleus accumbens, or cingulate cortex) (David et al., 2009); (Micheli, Ceccarelli, D'Andrea, & Tirone, 2018). The use of additional pharmacological or genetic methods to modulate adult neurogenesis and newborn neuron activity more specifically will help to get a deeper insight into the relation between AHN and the behavioural alterations of R451C Nlgn3 KI mice.

Overall, we describe for the first time the detrimental effect of the ASD-associated mutation R451C Nlgn3 on AHN and provide evidence that both social and neurogenesis deficits could be pharmacologically rescued. These data point to AHN manipulation as a potential therapeutic target to mitigate social deficits in some forms of ASDs and may open new avenues for the pharmacological treatment of these disorders.

Conflict of Interest

The authors declare no conflict of interest.

Author Contributions

E.C. and A.D.J. conceived the study and designed the experiments. R.G. and T.D. were responsible for animal handling. R.G. performed intraperitoneal BrdU animal injections and perfusion. R.G., S.F. and M.V. performed tissue cryosectioning, immunostaining and cell quantification. L.M., R.G. and F.T. performed confocal image acquisition. T.S and A.R. performed behavioural tests.
A.R., T.S., R.G, S.B., and E.C. performed statistical analysis. R.G. and E.C. wrote the first manuscript draft. A.D.J., A.R., G.L., S.B., Z.K., H.A., G.L., and E.C. critically revised the manuscript.
T.D. prepared Graphical Abstract
All authors contributed to data interpretation and approved the final version of the manuscript

Acknowledgments
This work was supported by grants from Sapienza University of Rome to EC, ADJ, and AR and by grants from the Swedish Research Council, and Swedish Brain Foundation to ZK.
The artwork was prepared using the freely available software BioRender and Servier Medical Art.
The authors acknowledge Dr Giulia Torromino for technical support

Data Accessibility Statement
The data that support the findings of this study will be openly available in a public repository

Figures and Figure Legends

Figure 1. Quantification of the number of immature and mature neurons in the DG of wild-type and knock-in mice.
A) Schematic representation of the experimental protocol: P42 mice were injected daily for five consecutive days (P42-P46) with BrdU and then sacrificed after two (P60) or eight (P106) weeks. **B**) Representative confocal 3D reconstruction from the Z-stack of a DG section from a WT mouse showing DCX (red) and BrdU (green) immunopositive cells, separately or as a merged; nuclei were labelled with Hoechst (blue). **C)** Quantification of $BrdU^+/DCX^+$ cells in the entire, dorsal or ventral DG of wild-type and knock-in mice. Note that a significant reduction in the number of $BrdU^+/DCX^+$ neurons was restricted to the ventral DG of KI with respect to the WT (whole DG: WT 1509±85.98, n=7; KI 1169±175.5, n=7; $p \geq 0.05$; dorsal DG: WT 702.8 ± 63.89, n=7; KI 578.4±90.76, n=7*;* $p \geq 0.05$; ventral DG: WT 848. ±57.99, n=7; KI 606.7±91.98, n=7*;* $p \leq 0.05$ **D)** Representative confocal image of a WT DG section double-stained for BrdU (red), and NeuN (green) **E)** Quantification of the BrdU/NeuN double-positive cells in the whole, dorsal and ventral DG of the hippocampus of wild-type and knock-in mice two weeks after the last BrdU injection. Note that only in the ventral DG there was a significant reduction in the number of adult-born neurons in KI with respect to

WT mice (whole DG: WT 4085±363.3, KI 3153±227.2, $p \leq 0,05$; dorsal DG: WT 1973±163.8, KI 1691±163.4, $p \geq 0,05$; ventral DG: WT 2143±207.4, n=7; KI 1433 ± 100, $p \leq 0.01$; n=7; **F)** Quantification of $BrdU^+/NeuN^+$cells in the whole, dorsal and ventral DG of the hippocampus of wild-type and knock-in mice sacrificed 8 weeks after the last BrdU injection (P106). The reduction of BrdU/NeuN double-positive neurons was only found in the ventral DG of KI with respect to WT mice ($BrdU^+/NeuN^+$ cells whole DG: WT 1716 ± 324,9, n=3; KI 1495 ± 332,5, n=3. *p≥0,05*; dorsal DG: WT 953,1 ± 313, n=3; KI 904,3 ± 261,7, n=3, *p≥0,05*; ventral DG: WT 803,9 ± 37,35, n=3; KI 563 ± 77,5, n=3 *p≤0,05*. *Student's t-test * p≤0.05*. Values are expressed as means ±SEM. Scale bar 50 µm.

Figure 2. Quantification of the number of quiescent and proliferating neural stem progenitor cells in the DG of wild-type and knock-in mice.

A) Representative confocal image, with orthogonal projections of triple-positive cells showing co-expression of GFAP (red), Ki67 (green) and Sox2 (blue). **B**) Quantification of $Sox2^+/GFAP^+/ Ki67^-$ quiescent NSCs (whole DG: WT 4555±251.8; KI 4359±241.8; dorsal DG: WT 1911±147.4; KI 2110±80.09*;* ventral DG: WT 2715±382.7; KI 2266±209.6; n=3,*ns p>0.05*); **C**) Quantification of $Sox2^+/GFAP^+/Ki67^+$ activated NSCs (whole DG: WT 447.1±56.14; KI 342.9±67.53; dorsal DG: WT 212.9±24.73; KI 157.1±28.16, *p>0.05*; ventral DG: WT 238.2±40.61; KI 190.1±44.27; n=3, *ns p>0.05*; **D**) Quantification of $Sox2^+/GFAP^-/Ki67^+$ Type 2a progenitor cells (whole DG: WT 576.6±72.61; KI 570.6±63.12; dorsal DG: WT 256.2±37.16*;* KI 280.9±31.98; ventral DG: WT 332.8±35.77, n=3; KI 291±32.25, n=3, *ns p>0.05*). **E**) Representative confocal images with orthogonal projections of cells co-labeled for DCX (red) and Ki67 (green). Cell nuclei were labeled with Hoechst (blue). Scale bars 50 µm. **F**) Quantification of $Ki67^+/DCX^+$ Type 2b/Type 3 neuroblasts (whole DG: WT 1083±58.26; 791.± 47.72; dorsal DG: WT 502.1±36.3; KI 355.5±50*;* ventral DG: WT 575.8±27.36; 429.8±22.17; n=7; *Student's t-test * p≤0.05 **p≤0.01*). Note that neuroblasts are reduced in KI with respect to WT mice.

Figure 3. Quantification of adult-born neurons formed in the DG of wild-type and knock-in mice after fluoxetine treatment.

A) Scheme of the experimental protocol. Quantification of BrdU/NeuN positive cells in the **B)** dorsal and **C)** ventral DG of wild-type and knock-in mice. There is a significant reduction of BrdU/NeuN positive neurons in KI VEH with respect to WT VEH mice in the ventral but not in the dorsal DG. The number of BrdU/NeuN cells in KI mice treated with fluoxetine increased, approximating that of WT VEH-treated and WT FLX-treated mice. Despite a robust increase in BrdU/NeuN positive cells in the FLX-treated KI mice, no difference was found with respect to the KI VEH-treated mice. **D**) Percentage ratio of $BrdU^+/NeuN^+$ on BrdU positive cells in the dorsal DG was unaffected in both KI and WT mice. **E**) Percentage of $BrdU^+/NeuN^+$ out of BrdU positive cells in the ventral DG. The differentiation rate was significantly increased in KI FLX-treated with respect to KI VEH mice (Kruskal-Wallis test $p \leq 0.05$, post-hoc Dunn's test: KI VEH vs KI FLX $p<0.05$).

Figure 4. Analysis of sociability and social novelty preference during the three-chamber behavioural test in wild-type and knock-in mice treated with fluoxetine and vehicle.

Social behaviour was studied by analysing the following parameters: time sniffing the object/stranger or the familiar/novel stranger (**A, D**); time spent in the three chambers (**B, E**); latency to the first entry (**C, F**).

Sociability analysis: **A)** time sniffing (chamber $F(1,32)=26.83$ $p\leq0.0001$; genotype $F(1,32)=5.14$ $p\leq0.05$; treatment $F(1,32)=0.09$ $p>0.05$; treatment*genotype $F(1,32)= 3.65$ $p=0.06$; object WT VEH vs stranger WT VEH $p\leq0.01$ object KI VEH vs stranger KI VEH $p>0.05$; stranger WT VEH vs stranger KI VEH $p\leq0.01$; stranger KI VEH vs stranger KI FLX $p\leq0.05$; object KI FLX vs stranger KI FLX $p\leq0.01$ with post-hoc LSD's test). **B)** Time in the chamber (chamber $F(2,64)=41$ $p<0.0001$; chamber*genotype $F(2,64)=3,25$ $p\leq0.05$; chamber*treatment*genotype $F(2,64)=3$ $p=0.06$; object chamber KI VEH vs stranger chamber KI VEH $p\leq0.01$; stranger chamber KI VEH vs stranger chamber WT VEH $p\leq0.01$; strange chamber KI FLX vs stranger chamber KI VEH $p\leq0.01$; center chamber KI FLX vs center chamber KI VEH $p\leq0.05$ with LSD's test). **C)** Latency to the first entry (treatment $F(1,32)=5.37$ $p\leq0.02$; stranger*genotype $F(1,32)=6.56$ $p\leq0.01$; stranger KI VEH vs stranger WT VEH $p<0.05$, stranger KI VEH vs stranger KI FLX $p<0.05$, LSD's test.

Social novelty preference analysis: **D)** time sniffing novelty $F(1,32)= 49.2$ $p<0.0001$; chamber time: chamber $F(2,64)=106$ $p<0.0001$treatment $F(1,32)=1.9$ $p>0.05$; genotype $F(1,32)=0.58$ $p>0.05$). **E)** Time in chamber (chamber $F(2,64)=106$ $p<0.0001$; treatment $F(1,32)=0.3$ $p>0.05$; genotype $F(1,32)=0.02$ $p>0.05$). **F)** Latency to first entry (treatment $F(1,32)= 0.01$, $p>0.05$; genotype $F(1,32)=1.81$ $p>0.05$). n=9; * $p\leq0.05$, ** $p\leq0.01$ LSD's test.

Figure 5. Quantification of activated newborn neurons immediately after the three-chamber behavioural test in animals treated with fluoxetine and vehicle.

A) Active adult-born neurons were identified by immunohistochemical detection of BrdU/c-Fos double-positive cells in free-floating DG containing sections obtained from mice sacrificed 1 hour after the end of the three-chamber behavioural tests**. B-C-D)** Quantification of the number of activated newborn neurons in the DG. **B)** ventral DG: the number of $BrdU^+/c\text{-}Fos^+$ cells increased in KI FLX with respect to KI VEH. This number even exceeds that of WT mice. Treatment $F(1,23)= 4.1$ $p\leq0.05$; KI FLX vs KI VEH $p\leq0.05$, KI FLX vs WT VEH $p\leq0.05$, LSD's test. **C)** Dorsal DG: the number of $BrdU^+/c\text{-}Fos^+$ cells was lower in KI VEH than in WT VEH mice. Fluoxetine treatment increased $BrdU^+/c\text{-}Fos^+$ cells in KI, while decreased their number in WT mice. Genotype X treatment interaction. $F(1,23)=14.54$ $p<0.001$*; WT VEH vs KI VEH p≤0.001, KI VEH vs KI FLX p≤0.05, LSD's test.* **D)** Whole DG: the number of $BrdU^+/c\text{-}Fos^+$ cells was reduced in KI VEH mice with respect to WT VEH. Fluoxetine increased $BrdU^+/c\text{-}Fos^+$ cells in KI mice with respect to the VEH treated group. Genotype X treatment interaction $F(1,23) =8.9$ $p<0.01$; WT VEH vs KI VEH $p\leq0.05$, KI VEH vs KI FLX $p\leq0.01$, LSD's test, n=7.* $p\leq0.05$, ** $p\leq0.01$, *** $p\leq0.001$, LSD's test.

Supporting information

Supplementary Figure 1. Coronal sections showing dorsal and ventral DG blocks.
Three-dimensional model (left top corner) of the hippocampus in the context of the whole mouse brain generated in BrainExplore (Lau *et al.,* 2008), a 3D application of the Allen Reference Atlas (www.brain-map.org), and 12 representative fluorescence images of 30-µm-thick brain coronal sections collected in 1 in 8 series, divided into dorsal (from #1 to #6) and ventral (from #7 to #12) DG; *scale bar 200µm*.

Supplementary figure 2. Quantification of proliferating BrdU⁺ and Ki67⁺ cells in the DG of wild-type and knock-in mice.
(**A**) Scheme of the experimental protocol: two-month-old mice were injected three times every two hours with BrdU and then sacrificed. (**B**) Quantification of BrdU⁺ cells in the whole, dorsal and ventral DG of the hippocampus of wild-type and knock-in mice did not reveal any difference in terms of proliferation (cell number in the whole DG: WT 2173 ± 257.4, n=7; KI 2273 ± 295.4, n=7; dorsal DG: WT 1083 ± 141.6, n=7; KI 1132 ± 156.2, n=7; ventral DG: WT 1120 ± 159.1, n=7; KI 1102 ± 116.4, n=7; *Student's t-test*, $p > 0.05$). (**C**)Quantification of Ki67⁺ cells in the whole, dorsal and ventral DG did not reveal any difference between wild-type and knock-in mice (Ki67⁺cells whole DG: WT 3710±385.6, KI 3421±421.7; dorsal DG: WT 1683±208.2, KI 1530±236.7; ventral DG: WT 2073±233.2, KI 1892±241.3; n=7; p>0.05, *Student's t-test).*

Supplementary Figure 3. Locomotor activity in vehicle- or fluoxetine-injected WT and KI mice during the three-chamber behavioural test.
A) Sociability session analysis: distance travelled (genotype $F(1,32)=6.65$ $p \leq 0.01$; chamber $F(2,64)=26.57$ $p \leq 0.0001$; chamber*genotype $F(2,64)=4.94$ $p \leq 0.01$; object chamber KI VEH vs object chamber WT VEH $p \leq 0.05$; object chamber WT FLX vs object chamber KI FLX $p \leq 0.01$; stranger chamber KI VEH vs stranger chamber KI FLX $p \leq 0.05$ with LSD's test). B) Social novelty preference analysis: distance travelled (genotype $F(1,32)=11.2$ $p<0.01$; chamber $F(2,64)=37.3$ $p<0.0001$); * $p \leq 0.05$, ** $p \leq 0.01$ LSD's test.

Supplementary figure 4. Immunohistochemical detection of dentate gyrus active mature neurons.
A) Representative confocal images of the DG of WT VEH mice, with orthogonal projections from Z-stacks showing active neurons co-expressing c-Fos (red) and NeuN (green), The staining confirms that the c-Fos positive cells were post-mitotic mature neurons.

Bibliography

Alenina, N., & Klempin, F. (2015). The role of serotonin in adult hippocampal neurogenesis. *Behavioural Brain Research*, *277*, 49–57.

Aman, M. G., Lam, K. S. L., & Van Bourgondien, M. E. (2005). Medication patterns in patients with autism: temporal, regional, and demographic influences. *Journal of Child and Adolescent Psychopharmacology*, *15*(1), 116–126.

Amiri, A., Cho, W., Zhou, J., Birnbaum, S. G., Sinton, C. M., McKay, R. M., & Parada, L. F. (2012). Pten deletion in adult hippocampal neural stem/progenitor cells causes cellular abnormalities and alters neurogenesis. *The Journal of Neuroscience*, *32*(17), 5880–

5890.
Anacker, C., & Hen, R. (2017). Adult hippocampal neurogenesis and cognitive flexibility - linking memory and mood. *Nature Reviews. Neuroscience*, *18*(6), 335–346.
Anacker, C., Luna, V. M., Stevens, G. S., Millette, A., Shores, R., Jimenez, J. C., Chen, B., et al. (2018). Hippocampal neurogenesis confers stress resilience by inhibiting the ventral dentate gyrus. *Nature*, *559*(7712), 98–102.
Bariselli, S., Hörnberg, H., Prévost-Solié, C., Musardo, S., Hatstatt-Burklé, L., Scheiffele, P., & Bellone, C. (2018). Role of VTA dopamine neurons and neuroligin 3 in sociability traits related to nonfamiliar conspecific interaction. *Nature Communications*, *9*(1), 3173.
Bernstein, H. L., Lu, Y.-L., Botterill, J. J., & Scharfman, H. E. (2019). Novelty and Novel Objects Increase c-Fos Immunoreactivity in Mossy Cells in the Mouse Dentate Gyrus. *Neural plasticity*, *2019*, 1815371.
Bicker, F., Nardi, L., Maier, J., Vasic, V., & Schmeisser, M. J. (2021). Criss-crossing autism spectrum disorder and adult neurogenesis. *Journal of Neurochemistry*, *159*(3), 452–478.
Budreck, E. C., & Scheiffele, P. (2007). Neuroligin-3 is a neuronal adhesion protein at GABAergic and glutamatergic synapses. *The European Journal of Neuroscience*, *26*(7), 1738–1748.
Burrows, E. L., Laskaris, L., Koyama, L., Churilov, L., Bornstein, J. C., Hill-Yardin, E. L., & Hannan, A. J. (2015). A neuroligin-3 mutation implicated in autism causes abnormal aggression and increases repetitive behavior in mice. *Molecular autism*, *6*, 62.
Cai, Y., Zhong, H., Li, X., Xiao, R., Wang, L., & Fan, X. (2019). The liver X receptor agonist TO901317 ameliorates behavioral deficits in two mouse models of autism. *Frontiers in Cellular Neuroscience*, *13*, 213.
Cameron, H. A., & Glover, L. R. (2015). Adult neurogenesis: beyond learning and memory. *Annual Review of Psychology*, *66*, 53–81.
Catavero, C., Bao, H., & Song, J. (2018). Neural mechanisms underlying GABAergic regulation of adult hippocampal neurogenesis. *Cell and Tissue Research*, *371*(1), 33–46.
Chadman, K. K., Gong, S., Scattoni, M. L., Boltuck, S. E., Gandhy, S. U., Heintz, N., & Crawley, J. N. (2008). Minimal aberrant behavioral phenotypes of neuroligin-3 R451C knockin mice. *Autism research : official journal of the International Society for Autism Research*, *1*(3), 147–158.
Chadman, K. K. (2011). Fluoxetine but not risperidone increases sociability in the BTBR mouse model of autism. *Pharmacology, Biochemistry, and Behavior*, *97*(3), 586–594.
Chubykin, A. A., Atasoy, D., Etherton, M. R., Brose, N., Kavalali, E. T., Gibson, J. R., & Südhof, T. C. (2007). Activity-dependent validation of excitatory versus inhibitory synapses by neuroligin-1 versus neuroligin-2. *Neuron*, *54*(6), 919–931.
Cope, E. C., Briones, B. A., Brockett, A. T., Martinez, S., Vigneron, P.-A., Opendak, M., Wang, S. S.-H., et al. (2016). Immature neurons and radial glia, but not astrocytes or microglia, are altered in adult cntnap2 and shank3 mice, models of autism. *eNeuro*, *3*(5).
David, D. J., Samuels, B. A., Rainer, Q., Wang, J.-W., Marsteller, D., Mendez, I., Drew, M., et al. (2009). Neurogenesis-dependent and -independent effects of fluoxetine in an animal model of anxiety/depression. *Neuron*, *62*(4), 479–493.
Ellegood, J., & Crawley, J. N. (2015). Behavioral and neuroanatomical phenotypes in mouse models of autism. *Neurotherapeutics*, *12*(3), 521–533.
Etherton, M., Földy, C., Sharma, M., Tabuchi, K., Liu, X., Shamloo, M., Malenka, R. C., et al.

(2011). Autism-linked neuroligin-3 R451C mutation differentially alters hippocampal and cortical synaptic function. *Proceedings of the National Academy of Sciences of the United States of America*, *108*(33), 13764–13769.

Fanselow, M. S., & Dong, H.-W. (2010). Are the dorsal and ventral hippocampus functionally distinct structures? *Neuron*, *65*(1), 7–19.

Gage, F. H., & Thompson, R. G. (1980). Differential distribution of norepinephrine and serotonin along the dorsal-ventral axis of the hippocampal formation. *Brain Research Bulletin*, *5*(6), 771–773.

Goh, S., & Peterson, B. S. (2012). Imaging evidence for disturbances in multiple learning and memory systems in persons with autism spectrum disorders. *Developmental Medicine and Child Neurology*, *54*(3), 208–213.

Gould, E., Beylin, A., Tanapat, P., Reeves, A., & Shors, T. J. (1999). Learning enhances adult neurogenesis in the hippocampal formation. *Nature Neuroscience*, *2*(3), 260–265.

Guzowski, J. F., Timlin, J. A., Roysam, B., McNaughton, B. L., Worley, P. F., & Barnes, C. A. (2005). Mapping behaviorally relevant neural circuits with immediate-early gene expression. *Current Opinion in Neurobiology*, *15*(5), 599–606.

Hill, A. S., Sahay, A., & Hen, R. (2015). Increasing Adult Hippocampal Neurogenesis is Sufficient to Reduce Anxiety and Depression-Like Behaviors. *Neuropsychopharmacology*, *40*(10), 2368–2378.

Jamain, S., Quach, H., Betancur, C., Råstam, M., Colineaux, C., Gillberg, I. C., Soderstrom, H., et al. (2003). Mutations of the X-linked genes encoding neuroligins NLGN3 and NLGN4 are associated with autism. *Nature Genetics*, *34*(1), 27–29.

Jaramillo, T. C., Liu, S., Pettersen, A., Birnbaum, S. G., & Powell, C. M. (2014). Autism-related neuroligin-3 mutation alters social behavior and spatial learning. *Autism research : official journal of the International Society for Autism Research*, *7*(2), 264–272.

Jessberger, S., & Gage, F. H. (2014). Adult neurogenesis: bridging the gap between mice and humans. *Trends in Cell Biology*, *24*(10), 558–563.

Jessberger, S., Römer, B., Babu, H., & Kempermann, G. (2005). Seizures induce proliferation and dispersion of doublecortin-positive hippocampal progenitor cells. *Experimental Neurology*, *196*(2), 342–351.

Kang, E., Wen, Z., Song, H., Christian, K. M., & Ming, G.-L. (2016). Adult neurogenesis and psychiatric disorders. *Cold Spring Harbor Perspectives in Biology*, *8*(9).

Kempermann, G., Gage, F. H., Aigner, L., Song, H., Curtis, M. A., Thuret, S., Kuhn, H. G., et al. (2018). Human adult neurogenesis: evidence and remaining questions. *Cell Stem Cell*, *23*(1), 25–30.

Kempermann, G., Jessberger, S., Steiner, B., & Kronenberg, G. (2004). Milestones of neuronal development in the adult hippocampus. *Trends in Neurosciences*, *27*(8), 447–452.

Kheirbek, M. A., Drew, L. J., Burghardt, N. S., Costantini, D. O., Tannenholz, L., Ahmari, S. E., Zeng, H., et al. (2013). Differential control of learning and anxiety along the dorsoventral axis of the dentate gyrus. *Neuron*, *77*(5), 955–968.

Kovács, K. J. (1998). c-Fos as a transcription factor: a stressful (re)view from a functional map. *Neurochemistry International*, *33*(4), 287–297.

Krzisch, M., Fülling, C., Jabinet, L., Armida, J., Gebara, E., Cassé, F., Habbas, S., et al. (2017). Synaptic Adhesion Molecules Regulate the Integration of New Granule Neurons in the Postnatal Mouse Hippocampus and their Impact on Spatial Memory. *Cerebral Cortex*, *27*(8), 4048–4059.

Kuhn, H. G., Toda, T., & Gage, F. H. (2018). Adult Hippocampal Neurogenesis: A Coming-of-Age Story. *The Journal of Neuroscience*, *38*(49), 10401–10410.

Lazarov, O., Demars, M. P., Zhao, K. D. T., Ali, H. M., Grauzas, V., Kney, A., & Larson, J. (2012). Impaired survival of neural progenitor cells in dentate gyrus of adult mice lacking fMRP. *Hippocampus*, *22*(6), 1220–1224.

Luo, Y., Shan, G., Guo, W., Smrt, R. D., Johnson, E. B., Li, X., Pfeiffer, R. L., et al. (2010). Fragile x mental retardation protein regulates proliferation and differentiation of adult neural stem/progenitor cells. *PLoS Genetics*, *6*(4), e1000898.

Lupo, G., Gioia, R., Nisi, P. S., Biagioni, S., & Cacci, E. (2019). Molecular mechanisms of neurogenic aging in the adult mouse subventricular zone. *Journal of experimental neuroscience*, *13*, 1179069519829040.

Meyza, K. Z., Defensor, E. B., Jensen, A. L., Corley, M. J., Pearson, B. L., Pobbe, R. L. H., Bolivar, V. J., et al. (2013). The BTBR T+ tf/J mouse model for autism spectrum disorders-in search of biomarkers. *Behavioural Brain Research*, *251*, 25–34.

Micheli, L., Ceccarelli, M., D'Andrea, G., & Tirone, F. (2018). Depression and adult neurogenesis: Positive effects of the antidepressant fluoxetine and of physical exercise. *Brain Research Bulletin*, *143*, 181–193.

Micheli, L., Creanza, T. M., Ceccarelli, M., D'Andrea, G., Giacovazzo, G., Ancona, N., Coccurello, R., et al. (2021). Transcriptome Analysis in a Mouse Model of Premature Aging of Dentate Gyrus: Rescue of Alpha-Synuclein Deficit by Virus-Driven Expression or by Running Restores the Defective Neurogenesis. *Frontiers in cell and developmental biology*, *9*, 696684.

Murray, F., Smith, D. W., & Hutson, P. H. (2008). Chronic low dose corticosterone exposure decreased hippocampal cell proliferation, volume and induced anxiety and depression like behaviours in mice. *European Journal of Pharmacology*, *583*(1), 115–127.

Navailles, S., Hof, P. R., & Schmauss, C. (2008). Antidepressant drug-induced stimulation of mouse hippocampal neurogenesis is age-dependent and altered by early life stress. *The Journal of Comparative Neurology*, *509*(4), 372–381.

Opendak, M., Offit, L., Monari, P., Schoenfeld, T. J., Sonti, A. N., Cameron, H. A., & Gould, E. (2016). Lasting adaptations in social behavior produced by social disruption and inhibition of adult neurogenesis. *The Journal of Neuroscience*, *36*(26), 7027–7038.

Oswald, D. P., & Sonenklar, N. A. (2007). Medication use among children with autism spectrum disorders. *Journal of Child and Adolescent Psychopharmacology*, *17*(3), 348–355.

Payet, J. M., Burnie, E., Sathananthan, N. J., Russo, A. M., Lawther, A. J., Kent, S., Lowry, C. A., et al. (2018). Exposure to acute and chronic fluoxetine has differential effects on sociability and activity of serotonergic neurons in the dorsal raphe nucleus of juvenile male balb/c mice. *Neuroscience*, *386*, 1–15.

Perera, T. D., Dwork, A. J., Keegan, K. A., Thirumangalakudi, L., Lipira, C. M., Joyce, N., Lange, C., et al. (2011). Necessity of hippocampal neurogenesis for the therapeutic action of antidepressants in adult nonhuman primates. *Plos One*, *6*(4), e17600.

Polšek, D., Jagatic, T., Cepanec, M., Hof, P. R., & Simić, G. (2011). Recent developments in neuropathology of autism spectrum disorders. *Translational neuroscience*, *2*(3), 256–264.

Postema, M. C., van Rooij, D., Anagnostou, E., Arango, C., Auzias, G., Behrmann, M., Filho, G. B., et al. (2019). Altered structural brain asymmetry in autism spectrum disorder in a study of 54 datasets. *Nature Communications*, *10*(1), 4958.

Radley, J. J., & Jacobs, B. L. (2002). 5-HT1A receptor antagonist administration decreases

cell proliferation in the dentate gyrus. *Brain Research*, *955*(1–2), 264–267.

Rothwell, P. E., Fuccillo, M. V., Maxeiner, S., Hayton, S. J., Gokce, O., Lim, B. K., Fowler, S. C., et al. (2014). Autism-associated neuroligin-3 mutations commonly impair striatal circuits to boost repetitive behaviors. *Cell*, *158*(1), 198–212.

Sacco, R., Cacci, E., & Novarino, G. (2018). Neural stem cells in neuropsychiatric disorders. *Current Opinion in Neurobiology*, *48*, 131–138.

Sahay, A., & Hen, R. (2007). Adult hippocampal neurogenesis in depression. *Nature Neuroscience*, *10*(9), 1110–1115.

Santarelli, L., Saxe, M., Gross, C., Surget, A., Battaglia, F., Dulawa, S., Weisstaub, N., et al. (2003). Requirement of hippocampal neurogenesis for the behavioral effects of antidepressants. *Science*, *301*(5634), 805–809.

Schnell, E., Bensen, A. L., Washburn, E. K., & Westbrook, G. L. (2012). Neuroligin-1 overexpression in newborn granule cells in vivo. *Plos One*, *7*(10), e48045.

Schnell, E., Long, T. H., Bensen, A. L., Washburn, E. K., & Westbrook, G. L. (2014). Neuroligin-1 knockdown reduces survival of adult-generated newborn hippocampal neurons. *Frontiers in Neuroscience*, *8*, 71.

Snyder, J. S., Soumier, A., Brewer, M., Pickel, J., & Cameron, H. A. (2011). Adult hippocampal neurogenesis buffers stress responses and depressive behaviour. *Nature*, *476*(7361), 458–461.

Stephenson, D. T., O'Neill, S. M., Narayan, S., Tiwari, A., Arnold, E., Samaroo, H. D., Du, F., et al. (2011). Histopathologic characterization of the BTBR mouse model of autistic-like behavior reveals selective changes in neurodevelopmental proteins and adult hippocampal neurogenesis. *Molecular autism*, *2*(1), 7.

Strange, B. A., Witter, M. P., Lein, E. S., & Moser, E. I. (2014). Functional organization of the hippocampal longitudinal axis. *Nature Reviews. Neuroscience*, *15*(10), 655–669.

Südhof, T. C. (2008). Neuroligins and neurexins link synaptic function to cognitive disease. *Nature*, *455*(7215), 903–911.

Surget, A., Tanti, A., Leonardo, E. D., Laugeray, A., Rainer, Q., Touma, C., Palme, R., et al. (2011). Antidepressants recruit new neurons to improve stress response regulation. *Molecular Psychiatry*, *16*(12), 1177–1188.

Tabuchi, K., Blundell, J., Etherton, M. R., Hammer, R. E., Liu, X., Powell, C. M., & Südhof, T. C. (2007). A neuroligin-3 mutation implicated in autism increases inhibitory synaptic transmission in mice. *Science*, *318*(5847), 71–76.

Taupin, P. (2007). BrdU immunohistochemistry for studying adult neurogenesis: paradigms, pitfalls, limitations, and validation. *Brain Research Reviews*, *53*(1), 198–214.

Toda, T., Parylak, S. L., Linker, S. B., & Gage, F. H. (2019). The role of adult hippocampal neurogenesis in brain health and disease. *Molecular Psychiatry*, *24*(1), 67–87.

Trobiani, L, Favaloro, F. L., Di Castro, M. A., Di Mattia, M., Cariello, M., Miranda, E., Canterini, S., et al. (2018). UPR activation specifically modulates glutamate neurotransmission in the cerebellum of a mouse model of autism. *Neurobiology of Disease*, *120*, 139–150.

Trobiani, Laura, Meringolo, M., Diamanti, T., Bourne, Y., Marchot, P., Martella, G., Dini, L., et al. (2020). The neuroligins and the synaptic pathway in Autism Spectrum Disorder. *Neuroscience and Biobehavioral Reviews*, *119*, 37–51.

Tunc-Ozcan, E., Peng, C.-Y., Zhu, Y., Dunlop, S. R., Contractor, A., & Kessler, J. A. (2019). Activating newborn neurons suppresses depression and anxiety-like behaviors. *Nature Communications*, *10*(1), 3768.

Uutela, M., Lindholm, J., Rantamäki, T., Umemori, J., Hunter, K., Võikar, V., & Castrén, M. L.

(2014). Distinctive behavioral and cellular responses to fluoxetine in the mouse model for Fragile X syndrome. *Frontiers in Cellular Neuroscience*, *8*, 150.

Varoqueaux, F., Jamain, S., & Brose, N. (2004). Neuroligin 2 is exclusively localized to inhibitory synapses. *European Journal of Cell Biology*, *83*(9), 449–456.

Xu, J., Du, Y.-L., Xu, J.-W., Hu, X.-G., Gu, L.-F., Li, X.-M., Hu, P.-H., et al. (2019). Neuroligin 3 regulates dendritic outgrowth by modulating akt/mtor signaling. *Frontiers in Cellular Neuroscience*, *13*, 518.

Yun, S., Reynolds, R. P., Petrof, I., White, A., Rivera, P. D., Segev, A., Gibson, A. D., et al. (2018). Stimulation of entorhinal cortex-dentate gyrus circuitry is antidepressive. *Nature Medicine*, *24*(5), 658–666.

Zhao, C., Deng, W., & Gage, F. H. (2008). Mechanisms and functional implications of adult neurogenesis. *Cell*, *132*(4), 645–660.

Zhou, Q.-G., Lee, D., Ro, E. J., & Suh, H. (2016). Regional-specific effect of fluoxetine on rapidly dividing progenitors along the dorsoventral axis of the hippocampus. *Scientific Reports*, *6*, 35572.

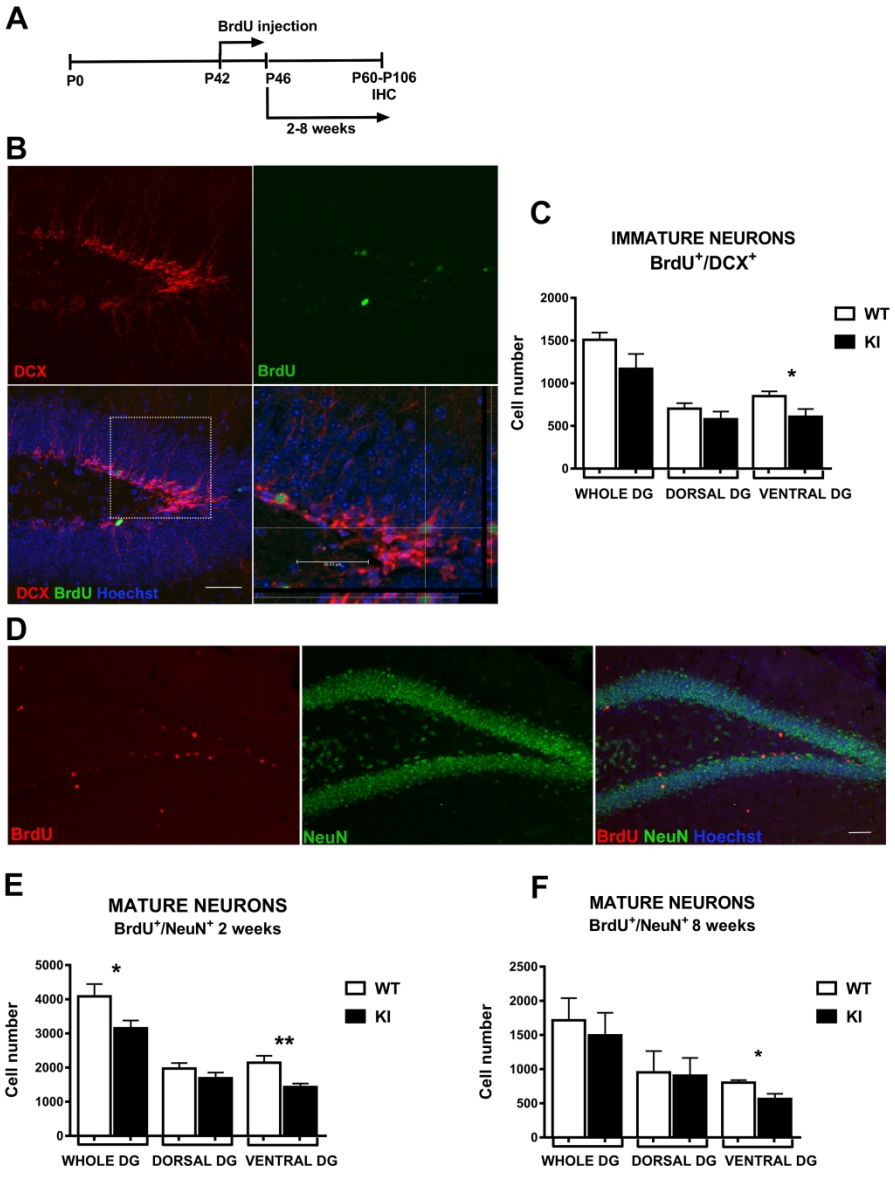

Figure 1. Quantification of the number of immature and mature neurons in the DG of wild-type and knock-in mice.

A) Schematic representation of the experimental protocol: P42 mice were injected daily for five consecutive days (P42-P46) with BrdU and then sacrificed after two (P60) or eight (P106) weeks. B) Representative confocal 3D reconstruction from the Z-stack of a DG section from a WT mouse showing DCX (red) and BrdU (green) immunopositive cells, separately or as a merged; nuclei were labelled with Hoechst (blue). C) Quantification of BrdU+/DCX+ cells in the entire, dorsal or ventral DG of wild-type and knock-in mice. Note that a significant reduction in the number of BrdU+/DCX+ neurons was restricted to the ventral DG of KI with respect to the WT (whole DG: WT 1509±85.98, n=7; KI 1169±175.5, n=7; $p \geq 0.05$; dorsal DG: WT 702.8 ± 63.89, n=7; KI 578.4±90.76, n=7; $p \geq 0.05$; ventral DG: WT 848. ±57.99, n=7; KI 606.7±91.98, n=7; $p \leq 0.05$ D) Representative confocal image of a WT DG section double-stained for BrdU (red), and NeuN (green) E) Quantification of the BrdU/NeuN double-positive cells in the whole, dorsal and ventral DG of the hippocampus of wild-type and knock-in mice two weeks after the last BrdU injection. Note that only in the ventral DG there was a significant reduction in the number of adult-born neurons in KI with respect to WT

mice (whole DG: WT 4085±363.3, KI 3153±227.2, p≤0,05; dorsal DG: WT 1973±163.8, KI 1691±163.4, p≥0,05; ventral DG: WT 2143±207.4, n=7; KI 1433 ± 100, p≤0.01; n=7; F) Quantification of BrdU+/NeuN+cells in the whole, dorsal and ventral DG of the hippocampus of wild-type and knock-in mice sacrificed 8 weeks after the last BrdU injection (P106). The reduction of BrdU/NeuN double-positive neurons was only found in the ventral DG of KI with respect to WT mice (BrdU+/NeuN+ cells whole DG: WT 1716 ± 324,9, n=3; KI 1495 ± 332,5, n=3. p≥0,05; dorsal DG: WT 953,1 ± 313, n=3; KI 904,3 ± 261,7, n=3, p≥0,05; ventral DG: WT 803,9 ± 37,35, n=3; KI 563 ± 77,5, n=3 p≤0,05. Student's t-test * p≤0.05. Values are expressed as means ±SEM. Scale bar 50 μm.

247x323mm (300 x 300 DPI)

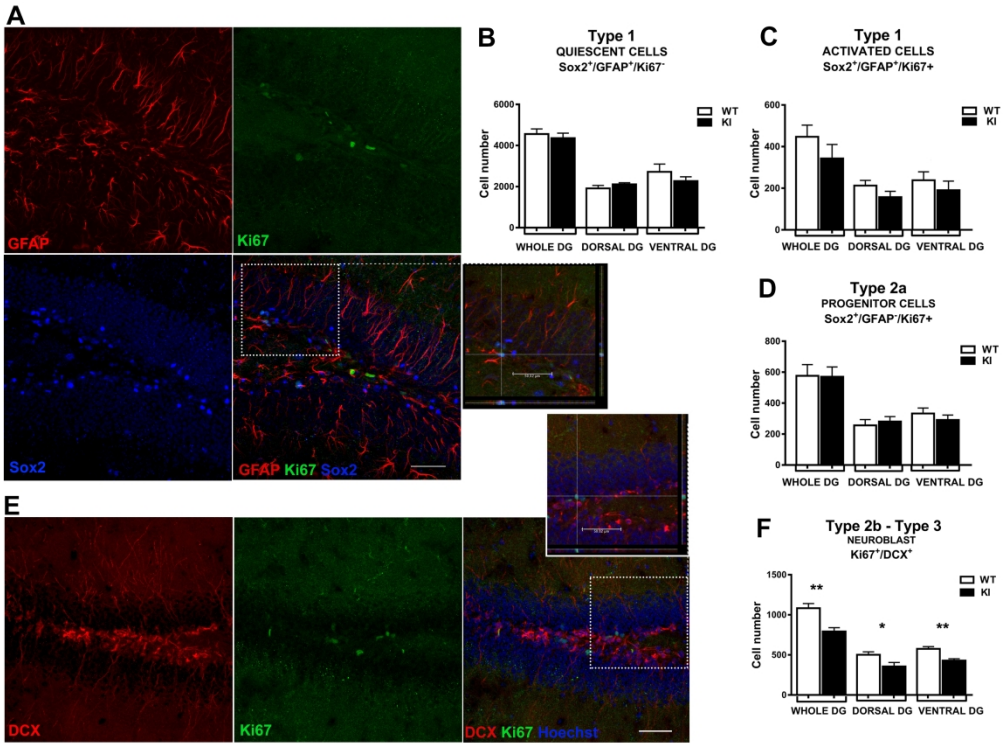

Figure 2. Quantification of the number of quiescent and proliferating neural stem progenitor cells in the DG of wild-type and knock-in mice.

A) Representative confocal image, with orthogonal projections of triple-positive cells showing co-expression of GFAP (red), Ki67 (green) and Sox2 (blue). B) Quantification of Sox2+/GFAP+/ Ki67- quiescent NSCs (whole DG: WT 4555±251.8; KI 4359±241.8; dorsal DG: WT 1911±147.4; KI 2110±80.09; ventral DG: WT 2715±382.7; KI 2266±209.6; n=3,ns p>0.05); C) Quantification of Sox2+/GFAP+/Ki67+ activated NSCs (whole DG: WT 447.1±56.14; KI 342.9±67.53; dorsal DG: WT 212.9±24.73; KI 157.1±28.16, p>0.05; ventral DG: WT 238.2±40.61; KI 190.1±44.27; n=3, ns p>0.05; D) Quantification of Sox2+/GFAP-/Ki67+ Type 2a progenitor cells (whole DG: WT 576.6±72.61; KI 570.6±63.12; dorsal DG: WT 256.2±37.16; KI 280.9±31.98; ventral DG: WT 332.8±35.77, n=3; KI 291±32.25, n=3, ns p>0.05). E) Representative confocal images with orthogonal projections of cells co-labeled for DCX (red) and Ki67 (green). Cell nuclei were labeled with Hoechst (blue). Scale bars 50 μm. F) Quantification of Ki67+/DCX+ Type 2b/Type 3 neuroblasts (whole DG: WT 1083±58.26; 791.± 47.72; dorsal DG: WT 502.1±36.3; KI 355.5±50; ventral DG: WT 575.8±27.36; 429.8±22.17; n=7; Student's t-test * p≤0.05 **p≤0.01). Note that neuroblasts are reduced in KI with respect to WT mice.

323x240mm (300 x 300 DPI)

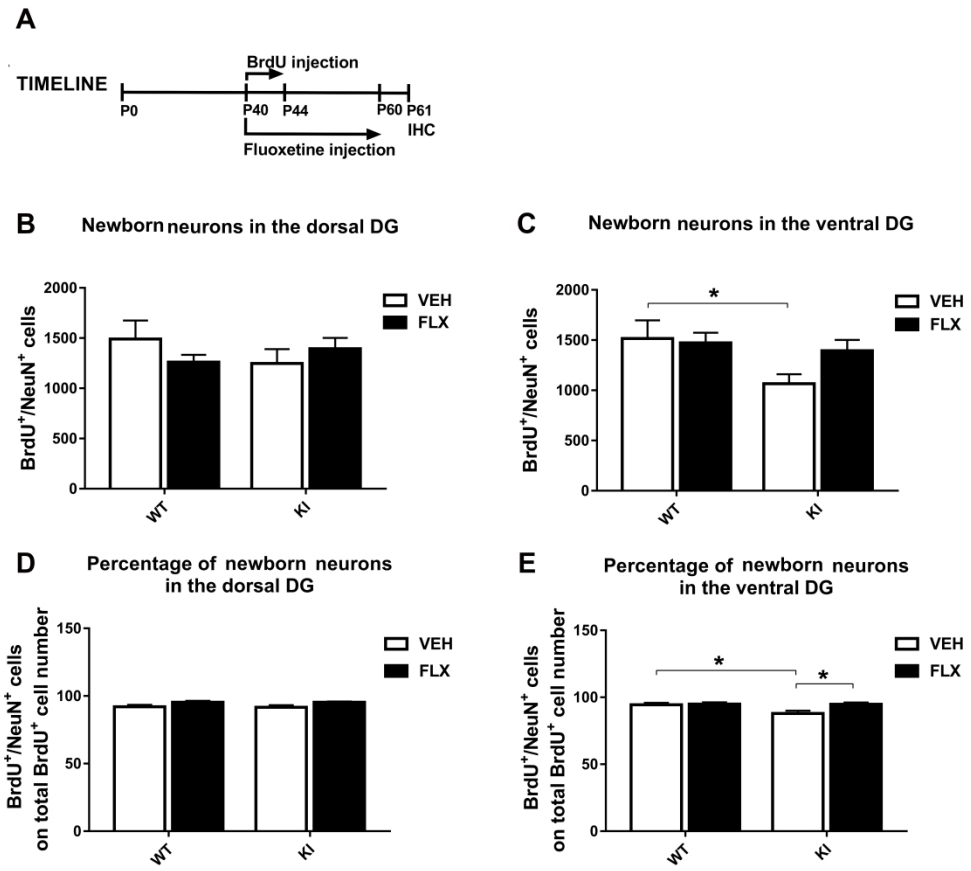

Figure 3. Quantification of adult-born neurons formed in the DG of wild-type and knock-in mice after fluoxetine treatment.
A) Scheme of the experimental protocol. Quantification of BrdU/NeuN positive cells in the B) dorsal and C) ventral DG of wild-type and knock-in mice. There is a significant reduction of BrdU/NeuN positive neurons in KI VEH with respect to WT VEH mice in the ventral but not in the dorsal DG. The number of BrdU/NeuN cells in KI mice treated with fluoxetine increased, approximating that of WT VEH-treated and WT FLX-treated mice. Despite a robust increase in BrdU/NeuN positive cells in the FLX-treated KI mice, no difference was found with respect to the KI VEH-treated mice. D) Percentage ratio of BrdU+/NeuN+ on BrdU positive cells in the dorsal DG was unaffected in both KI and WT mice. E) Percentage of BrdU+/NeuN+ out of BrdU positive cells in the ventral DG. The differentiation rate was significantly increased in KI FLX-treated with respect to KI VEH mice (Kruskal-Wallis test $p \leq 0.05$, post-hoc Dunn's test: KI VEH vs KI FLX $p < 0.05$).

253x224mm (600 x 600 DPI)

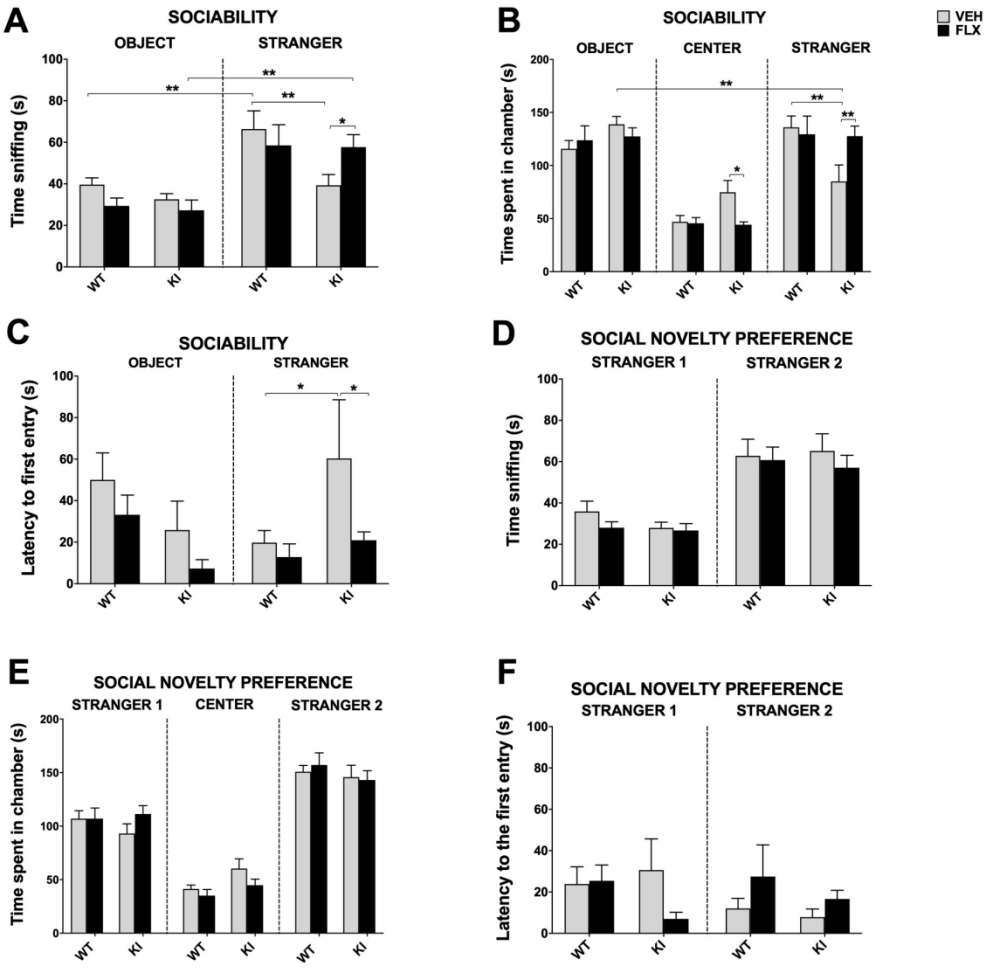

Figure 4. Analysis of sociability and social novelty preference during the three-chamber behavioural test in wild-type and knock-in mice treated with fluoxetine and vehicle.

Social behaviour was studied by analysing the following parameters: time sniffing the object/stranger or the familiar/novel stranger (A, D); time spent in the three chambers (B, E); latency to the first entry (C, F). Sociability analysis: A) time sniffing (chamber $F(1,32)=26.83$ $p\leq0.0001$; genotype $F(1,32)=5.14$ $p\leq0.05$; treatment $F(1,32)=0.09$ $p>0.05$; treatment*genotype $F(1,32)= 3.65$ $p=0.06$; object WT VEH vs stranger WT VEH $p\leq0.01$ object KI VEH vs stranger KI VEH $p>0.05$; stranger WT VEH vs stranger KI VEH $p\leq0.01$; stranger KI VEH vs stranger KI FLX $p\leq0.05$; object KI FLX vs stranger KI FLX $p\leq0.01$ with post-hoc LSD's test). B) Time in the chamber (chamber $F(2,64)=41$ $p<0.0001$; chamber*genotype $F(2,64)=3,25$ $p\leq0.05$; chamber*treatment*genotype $F(2,64)=3$ $p=0.06$; object chamber KI VEH vs stranger chamber KI VEH $p\leq0.01$; stranger chamber KI VEH vs stranger chamber WT VEH $p\leq0.01$; strange chamber KI FLX vs stranger chamber KI VEH $p\leq0.01$; center chamber KI FLX vs center chamber KI VEH $p\leq0.05$ with LSD's test). C) Latency to the first entry (treatment $F(1,32)=5.37$ $p\leq0.02$; stranger*genotype $F(1,32)=6.56$ $p\leq0.01$; stranger KI VEH vs stranger WT VEH $p<0.05$, stranger KI VEH vs stranger KI FLX $p<0.05$, LSD's test.

Social novelty preference analysis: D) time sniffing novelty $F(1,32)= 49.2$ $p<0.0001$; chamber time: chamber $F(2,64)=106$ $p<0.0001$treatment $F(1,32)=1.9$ $p>0.05$; genotype $F(1,32)=0.58$ $p>0.05$). E) Time in chamber (chamber $F(2,64)=106$ $p<0.0001$; treatment $F(1,32)=0.3$ $p>0.05$; genotype $F(1,32)=0.02$ $p>0.05$). F) Latency to first entry (treatment $F(1,32)= 0.01$, $p>0.05$; genotype $F(1,32)=1.81$ $p>0.05$). n=9; * $p\leq0.05$, ** $p\leq0.01$ LSD's test.

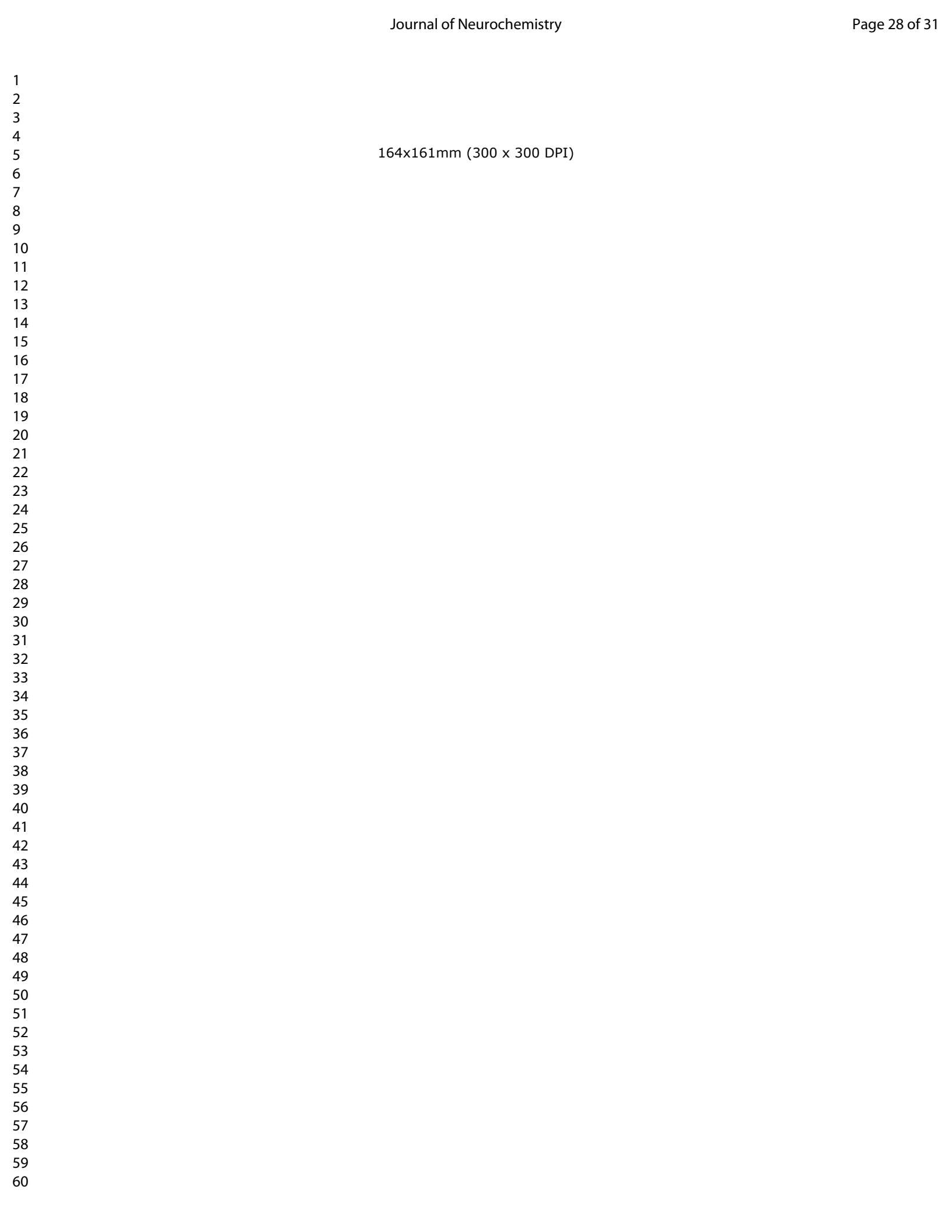
164x161mm (300 x 300 DPI)

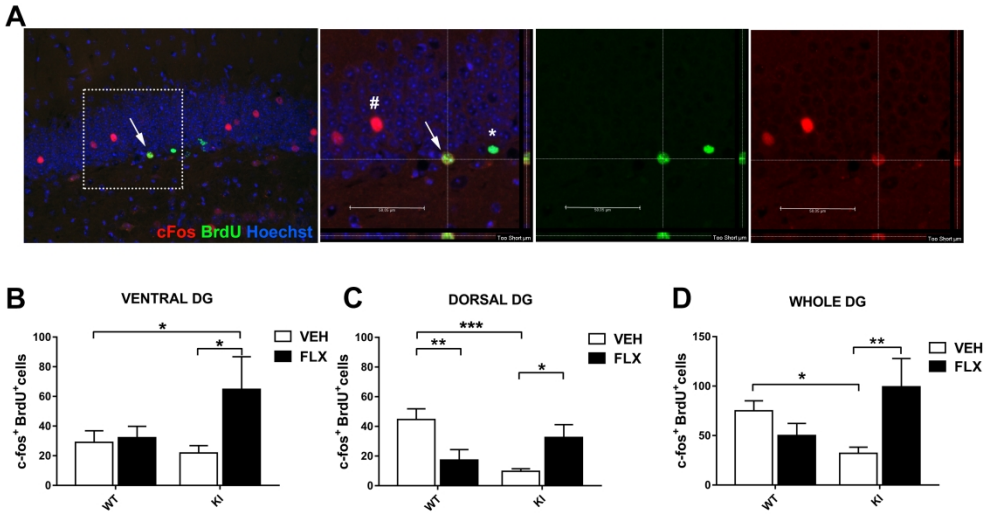

Figure 5. Quantification of activated newborn neurons immediately after the three-chamber behavioural test in animals treated with fluoxetine and vehicle.

A) Active adult-born neurons were identified by immunohistochemical detection of BrdU/c-Fos double-positive cells in free-floating DG containing sections obtained from mice sacrificed 1 hour after the end of the three-chamber behavioural tests. B-C-D) Quantification of the number of activated newborn neurons in the DG. B) ventral DG: the number of BrdU+/c-Fos+ cells increased in KI FLX with respect to KI VEH. This number even exceeds that of WT mice. Treatment $F(1,23)= 4.1$ $p\leq0.05$; KI FLX vs KI VEH $p\leq0.05$, KI FLX vs WT VEH $p\leq0.05$, LSD's test. C) Dorsal DG: the number of BrdU+/c-Fos+ cells was lower in KI VEH than in WT VEH mice. Fluoxetine treatment increased BrdU+/c-Fos+ cells in KI, while decreased their number in WT mice. Genotype X treatment interaction. $F(1,23)=14.54$ $p<0.001$; WT VEH vs KI VEH $p\leq0.001$, KI VEH vs KI FLX $p\leq0.05$, LSD's test. D) Whole DG: the number of BrdU+/c-Fos+ cells was reduced in KI VEH mice with respect to WT VEH. Fluoxetine increased BrdU+/c-Fos+ cells in KI mice with respect to the VEH treated group. Genotype X treatment interaction $F(1,23) =8.9$ $p<0.01$; WT VEH vs KI VEH $p\leq0.05$, KI VEH vs KI FLX $p\leq0.01$, LSD's test, n=7.* $p\leq0.05$, ** $p\leq0.01$, *** $p\leq0.001$, LSD's test.

294x234mm (300 x 300 DPI)

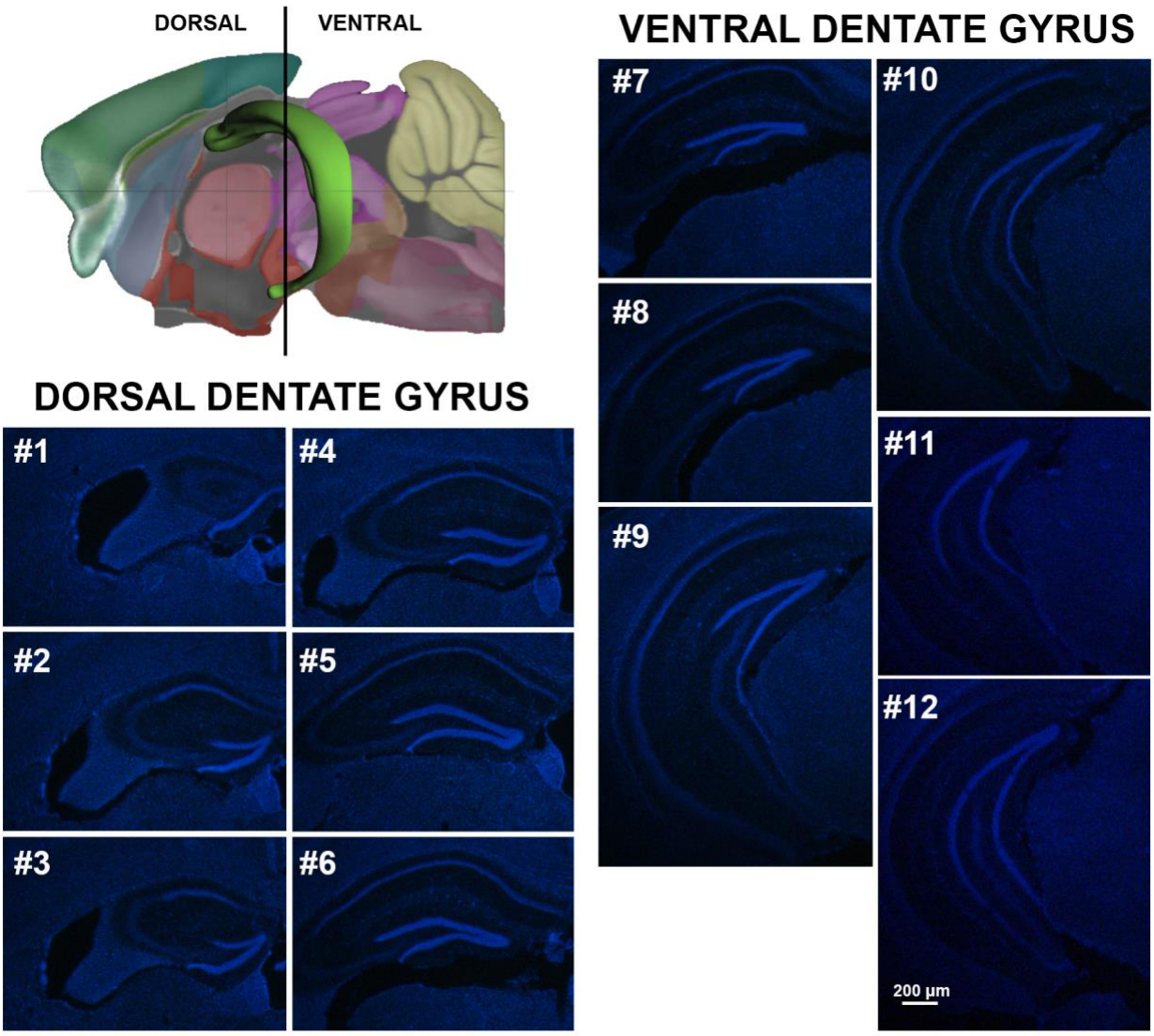

Supporting information

Supplementary Figure 1. Coronal sections showing dorsal and ventral DG blocks.

Three-dimensional model (left top corner) of the hippocampus in the context of the whole mouse brain generated in BrainExplore (Lau *et al.,* 2008), a 3D application of the Allen Reference Atlas (www.brain-map.org), and 12 representative fluorescence images of 30-µm-thick brain coronal sections collected in 1 in 8 series, divided into dorsal (from #1 to #6) and ventral (from #7 to #12) DG; *scale bar 200µm*.

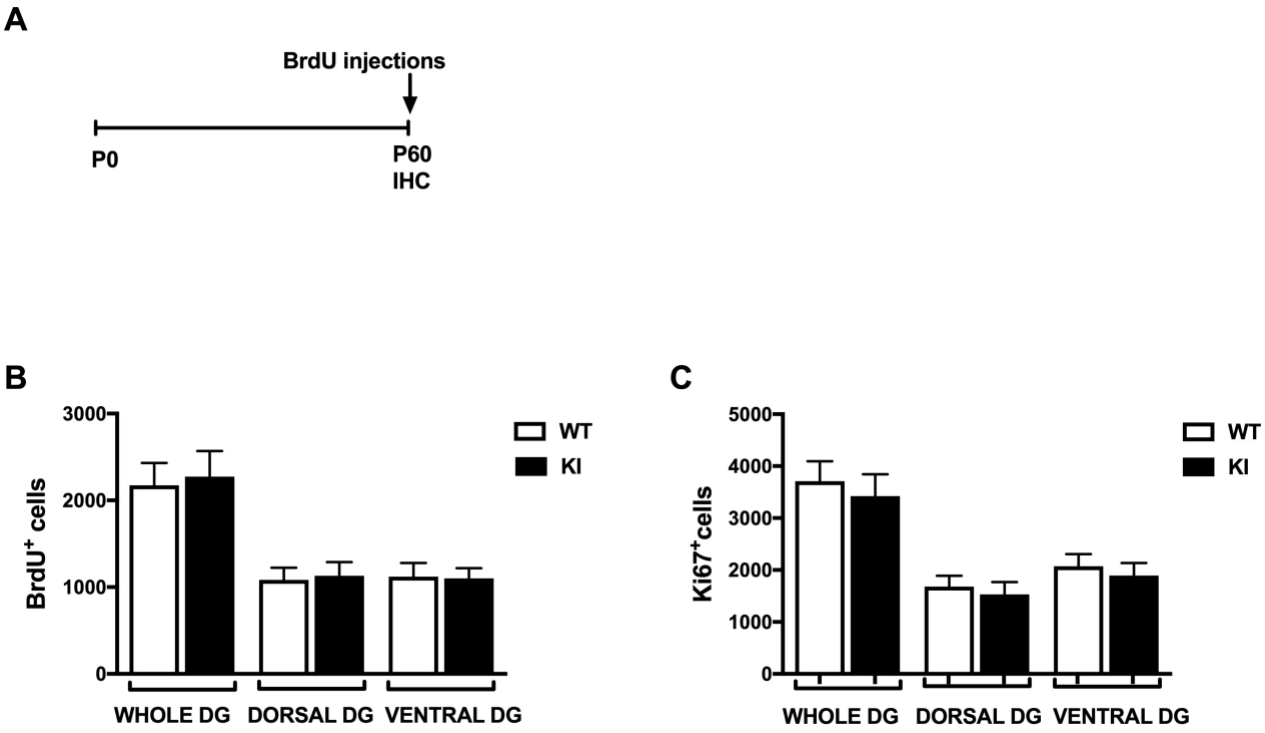

Supplementary figure 2. Quantification of proliferating BrdU$^+$ and Ki67$^+$ cells in the DG of wild-type and knock-in mice.

(**A**) Scheme of the experimental protocol: two-month-old mice were injected three times every two hours with BrdU and then sacrificed. (**B**) Quantification of BrdU$^+$ cells in the whole, dorsal and ventral DG of the hippocampus of wild-type and knock-in mice did not reveal any difference in terms of proliferation (cell number in the whole DG: WT 2173 ± 257.4, n=7; KI 2273 ± 295.4, n=7; dorsal DG: WT 1083 ± 141.6, n=7; KI 1132 ± 156.2, n=7; ventral DG: WT 1120 ± 159.1, n=7; KI 1102 ± 116.4, n=7; *Student's t-test*, $p > 0.05$). (**C**)Quantification of Ki67$^+$ cells in the whole, dorsal and ventral DG did not reveal any difference between wild-type and knock-in mice (Ki67$^+$cells whole DG: WT 3710±385.6, KI 3421±421.7; dorsal DG: WT 1683±208.2, KI 1530±236.7; ventral DG: WT 2073±233.2, KI 1892±241.3; n=7; p>0.05, *Student's t-test).*

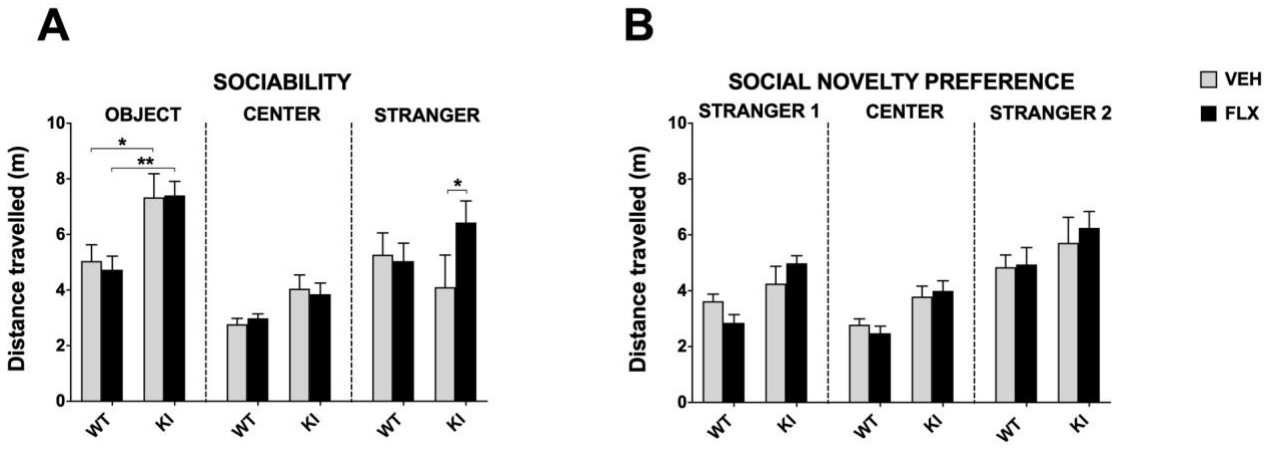

Supplementary Figure 3. Locomotor activity in vehicle- or fluoxetine-injected WT and KI mice during the three-chamber behavioural test.

A) Sociability session analysis: distance travelled (genotype $F(1,32)=6.65$ $p\leq0.01$; chamber $F(2,64)=26.57$ $p\leq0.0001$; chamber*genotype $F(2,64)=4.94$ $p\leq0.01$; object chamber KI VEH vs object chamber WT VEH $p\leq0.05$; object chamber WT FLX vs object chamber KI FLX $p\leq0.01$; stranger chamber KI VEH vs stranger chamber KI FLX $p\leq0.05$ with LSD's test). B) Social novelty preference analysis: distance travelled (genotype $F(1,32)=11.2$ $p<0.01$; chamber $F(2,64)=37.3$ $p<0.0001$); n=9; * $p\leq0.05$, ** $p\leq0.01$ LSD's test.

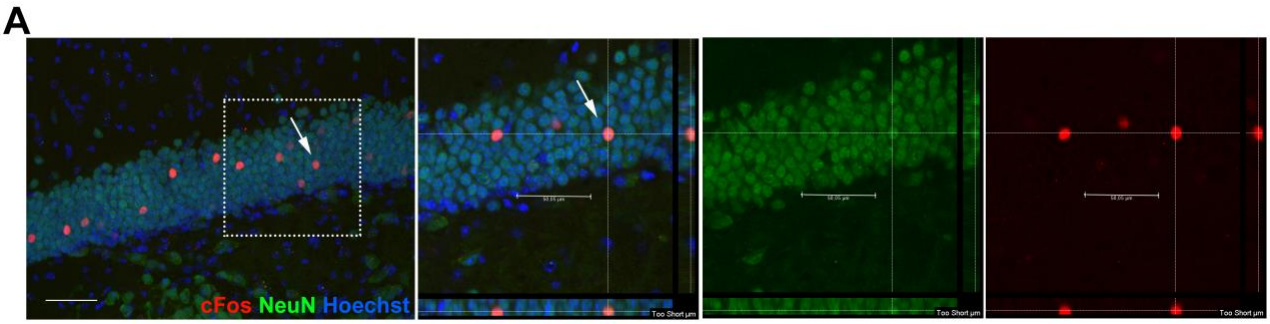

Supplementary figure 4. Immunohistochemical detection of dentate gyrus active mature neurons.

A) Representative confocal images of the DG of WT VEH mice, with orthogonal projections from Z-stacks showing active neurons co-expressing c-Fos (red) and NeuN (green), The staining confirms that the c-Fos positive cells were post-mitotic mature neurons.